Self-induced transparency solitary waves in a doped nonlinear photonic band gap material

Neşet Aközbek* and Sajeev John
Department of Physics, University of Toronto, 60 St. George Street, Toronto, Ontario, Canada M5S 1A7
(Received 11 February 1998)

We derive the properties of self-induced transparency (SIT) solitary waves in a one-dimensional periodic structure doped uniformly with resonance two-level atoms. In our model, the electromagnetic field is treated classically and the dopant atoms are described quantum mechanically. The resulting solitary waves take the form of ultrashort (picosecond) laser pulses which propagate near the band edge of the nonlinear photonic band gap (PBG) material doped with rare-earth atoms such as erbium. Solitary wave formation involves the combined effects of group velocity dispersion (GVD), nonresonant Kerr nonlinearity, and resonant interaction with dopant atoms. We derive the general Maxwell-Bloch equations for a nonlinear PBG system and then demonstrate the existence of elementary solitary wave solutions for frequencies far outside the gap where GVD effects are negligible and for frequencies near the photonic band edge where GVD effects are crucial. We find two distinct new types of propagating SIT solitary wave pulses. Far from Bragg resonance, we recapture the usual McCall-Hahn soliton with hyperbolic secant profile when the nonlinear Kerr coefficient $\chi^{(3)}=0$. However, when the host nonresonant Kerr coefficient is nonzero, we obtain the first new type of soliton. In this case, the optical soliton envelope function deviates from the hyperbolic secant profile and pulse propagation requires nontrivial phase modulation (chirping). We derive the dependence of the solitary wave structure on the Kerr coefficient $\chi^{(3)}$, the resonance impurity atom density, and the detuning of the average laser frequency from the atomic transition. When the laser frequency and the atomic transition frequencies are near the photonic band edge we obtain the second type of soliton. To illustrate the second type of soliton we consider two special cases. In the first case, GVD facilitates the propagation of an unchirped SIT-gap soliton moving at a velocity fixed by the material's parameters. The soliton structure changes dramatically as the laser frequency is tuned through the atomic resonance. In the second illustrative case we set the Kerr coefficient $\chi^{(3)}=0$. In this case, the solution is a chirped pulse which arises from the balance between GVD and the resonance interaction with the dopant atoms. Finally, we show that under certain circumstances, these solitary wave solutions may persist even in the presence of (subpicosecond) dipolar dephasing of the dopant atoms and absorption losses of the host PBG material, provided that the system is incoherently pumped. These results may be relevant to the application of PBG materials as optical devices in fiber-optic networks. [S1063-651X(98)08409-8]

PACS number(s): 42.70.Qs, 42.65.Tg, 42.50.Md

I. INTRODUCTION

Optical fiber solitons [1] have received considerable attention for more than a decade in the context of optical data transmission over long distances. The physical mechanism for the formation of a fiber soliton is the balance of group velocity dispersion (GVD) due to the frequency-dependent refractive index of the fiber and self-phase modulation due to the nonlinear Kerr effect [2]. More recently, it has been shown that optical gap solitons of a similar nature may exist in a nonlinear Bragg grating [3–7] and a nonlinear photonic band gap (PBG) material [8] in which GVD is provided by the periodic dielectric modulation of the underlying material. This is of particular importance for the application of PBG materials as optical interconnects in fiber-optic networks. In a PBG material, a frequency gap is opened in which there are no linear propagating electromagnetic modes for frequencies within the gap. Near a photonic band edge GVD is manifest even in the absence of a frequency-dependent refractive index and can be many orders of magnitude larger than found in conventional silica fibers.

Amplification and reshaping of an optical signal in a fiber is facilitated by passing the pulse through an active region doped with resonant atoms such as erbium. Unlike the optical solitons of a nonresonant Kerr medium, solitons in an active medium containing resonant two-level atoms involve the coherent absorption and reemission of light from the atoms in which the quantum mechanical Bloch vector of the atoms undergoes a 2π rotation. These solutions are referred to as self-induced transparency (SIT) solitons and were described by McCall and Hahn in 1967 [9]. They showed that under certain conditions a soliton pulse can propagate through a gas of resonant atoms, without distortion or attenuation. In the SIT soliton the role of material dispersion is replaced by the coherent absorption and subsequent stimulated emission of light into the direction of the incident laser pulse. The formation of the SIT soliton requires ultrashort high intensity pulses, which propagate on time scales short compared to the damping times of the Bloch vector determined by spontaneous emission and dipolar dephasing effects. Since their discovery, SIT solitons for two-level atoms in ordinary vacuum have received considerable attention [10–12].

Recently Nakazawa *et al.* [13] have observed self-induced

*Present address: Weapons Sciences Directorate, AMSAM-RD-WS-ST, U.S. Army Aviation and Missile Command, Redstone Arsenal, Alabama 35898.

transparency solitons in an erbium doped silica fiber waveguide. In their experiment, the fiber was cooled to a temperature of 4.2 K at which the dipole-dephasing time is of the order of nanoseconds. The SIT fiber solitons consisted of 500 picosecond laser pulses which are short enough to be in the coherent photon-atom interaction regime. Fibers doped with rare-earth atoms such as erbium, ytterbium, neodymium, and thulium have been studied for the purpose of pulse amplification. In particular, the erbium atom has a resonant transition near 1.55 μm, the wavelength of choice for optical telecommunications. It has been theoretically demonstrated that solitons may exist in an erbium doped fiber through the combined effects of the GVD, Kerr effects of the host medium, and the resonant interaction with atoms [14]. These solitons satisfy both the nonlinear Schrödinger equation (NLSE) as well as the atomic Bloch equations. Accordingly they are called SIT-NLS solitons. However, the existence of the SIT-NLS soliton requires a strict relation among the material parameters [14] which is difficult to satisfy in general. For example, given the Kerr coefficient of silica and dipole moment for the relevant erbium transition, the required GVD is many orders of magnitude larger than possible in most silica fibers.

In this paper we consider a one-dimensional nonlinear photonic band gap material (Bragg grating) doped uniformly with resonant two-level atoms. Systems of this nature are easily fabricated. It also provides a valuable paradigm for a doped, three-dimensional nonlinear PBG material exhibiting a complete three-dimensional gap. Previously, some specialized models of a doped Bragg grating have been considered which yield exact analytical solutions. Mantsyzov and Kuzmin [15] have studied pulse propagation in a *discrete* one-dimensional medium made of two-level atoms. This model was extended by Kozhekin and Kurizki [16] to a continuous medium in which thin layers of resonant atoms are placed at regular intervals inside the periodic dielectric medium. However, from a practical point of view, these systems are difficult to realize. In our uniformly doped PBG model we use the slowly varying envelope approximation (SVEA) to derive the Maxwell-Bloch equations for the forward and Bragg scattered electric field amplitudes. When the laser frequency is tuned close to the photonic band edge, we show that pulse propagation is described by an effective nonlinear Schrödinger equation coupled to the atomic Bloch equations. The combined effects of GVD and nonresonant Kerr effect of the host PBG material lead to a solitary wave which is simultaneously a gap soliton and a SIT soliton, which we refer to as a SIT-gap soliton. Although the underlying equations for the band-edge approximation are similar to those of the doped fiber, the physical meaning of these equations is very different. In the SIT-gap soliton, the time variable in the fiber soliton equation is replaced by a spatial coordinate. This is due to the fact that the GVD in fibers is provided by the frequency-dependent dielectric constant, whereas in a PBG the GVD arises from the periodic spatial variation of the dielectric constant. In contrast to the fiber SIT soliton, the SIT-gap soliton may be simpler to realize experimentally since it does not require a strict condition among the material parameters.

Using the model described above, we derive the existence of two distinct types of optical solitons. The first new type of soliton occurs when the laser frequency and the atomic transition frequency are near a photonic band edge. We illustrate this first type of soliton by focusing on two special cases, both of which lead to simple analytic results. The first special case is an unchirped soliton which travels at a velocity prescribed by the material parameters. This involves the full effect of GVD, nonresonant Kerr effect, and the resonant interaction with impurity atoms. This in turn leads to a new class of solitons moving with general velocities. However, this family of solitons involves self-phase modulation (chirping) as the velocity deviates from the prescribed velocity. The second illustrative case is that of a chirped soliton arising from band-edge GVD and resonant interaction with impurity atoms, but vanishing Kerr nonlinearity of the background dielectric material.

A second type of optical soliton arises when the laser field frequency is far outside the PBG. Here, we derive the SIT-Kerr soliton of a uniform medium. Such a solution has been considered by Matulic and Eberly [17] in the limit of a small Kerr coefficient. Here we obtain an exact solution, which cannot be extrapolated from the result of Matulic and Eberly. The exact solution exhibits self-phase modulation and is not a simple hyperbolic secant type envelope function. The soliton amplitude and pulse width depend on the Kerr coefficient and the dopant density. It reduces to the McCall-Hahn SIT soliton when the Kerr coefficient is set to zero.

These classical solitary wave solutions involve high intensity laser fields and are distinct from the quantum gap solitons [18] which arise from a quantum mechanical treatment of the electromagnetic field. The latter are highly nonclassical states of light and may involve only a small number of photons. The SIT solitary waves in the present paper involve a large number of photons in a classical (coherent) state.

II. MAXWELL-BLOCH EQUATIONS FOR A PERIODIC DIELECTRIC MEDIUM

We consider a one-dimensional periodic medium doped with two-level atoms. For intense optical pulses containing many photons, a semiclassical treatment of the radiation field is adequate. The coupled atom-field system is then described by the Maxwell-Bloch equations [19]. We consider a host medium in which the dielectric constant takes the form

$$\epsilon(x)=\tilde{\epsilon}+\Delta\epsilon\,\cos(2k_0x). \tag{2.1}$$

Here $\tilde{\epsilon}$ is the average dielectric constant of the medium, $\Delta\epsilon$ is the strength of the periodic dielectric variation ($\Delta\epsilon\ll\tilde{\epsilon}$), and $k_0=\pi/a_0$ for lattice constant a_0. In the case that the electric field is always perpendicular to the direction in which it varies, Maxwell's equations lead to the following scalar wave equation:

$$\frac{\partial^2E(x,t)}{\partial x^2}-\frac{\epsilon(x)}{c^2}\frac{\partial^2E(x,t)}{\partial t^2}-\frac{4\pi}{c^2}\frac{\partial^2P_{\rm nl}^{\rm host}(x,t)}{\partial t^2}-\frac{4\pi}{c^2}\frac{\partial^2P_{\rm nl}^{\rm atoms}(x,t)}{\partial t^2}=0. \tag{2.2}$$

Here $P_{\rm nl}^{\rm atoms}$ is the nonlinear polarization due to the two-level atoms and $P_{\rm nl}^{\rm host}$ is the nonresonant nonlinear contribution of

the host medium which is assumed to be of the form of a simple Kerr response: $P_{\rm nl}^{\rm host}=\chi^{(3)}|E|^2E$ where $\chi^{(3)}$ is the Kerr constant. Here we assume that all scattering of the ultrashort laser pulse by the atoms is in the forward direction. Since the periodic dielectric function can scatter light back and forth, the total electric field inside the periodic medium can be written in terms of forward and Bragg reflected field components:

$$E(x,t)=E_1(x,t)e^{-i\omega_0 t+ik_0 x}+E_2(x,t)e^{-i\omega_0 t-ik_0 x}+\text{c.c.}, \tag{2.3}$$

where ω_0 is the average frequency of the laser pulse. Likewise the polarization due to the two-level atoms is given by

$$P_{\rm nl}^{\rm atoms}(x,t)=P_1(x,t)e^{-i\omega_0 t+ik_0 x}+P_2(x,t)e^{-i\omega_0 t-ik_0 x}+\text{c.c.} \tag{2.4}$$

In Eqs. (2.3) and (2.4), E_1, E_2, P_1, and P_2 are slowly varying envelope functions. In the slowly varying envelope approximation [19] it is assumed that $|\partial E_{1,2}/\partial t|\ll\omega_0|E_{1,2}|$, $|\partial E_{1,2}/\partial x|\ll k_0|E_{1,2}|$ and that higher derivative terms with respect to x and t may be neglected. The dopant atoms are distributed uniformly but randomly in space with average density N_d. In this case, the atomic polarization of the atoms is represented as a continuous function of x. In particular, $P_{1,2}=N_d\langle p_{1,2}\rangle$, where $p_{1,2}$ are single-atom polarization operators which will be defined in terms of the atomic density matrix. Inserting Eqs. (2.3) and (2.4) into Eq. (2.2) with Eq. (2.1) we obtain

$$i\frac{\partial E_1}{\partial t}+i\frac{\partial E_1}{\partial x}+\beta E_2+n_L(|E_1|^2+2|E_2|^2)E_1+\eta\langle p_1\rangle=0, \tag{2.5}$$

$$i\frac{\partial E_2}{\partial t}-i\frac{\partial E_2}{\partial x}+\beta E_1+n_L(|E_2|^2+2|E_1|^2)E_2+\eta\langle p_2\rangle=0. \tag{2.6}$$

Here, x and t are dimensionless variables measured in units of k_0^{-1} and ω_0^{-1}, respectively. The other parameters are defined as $\omega_0=c\pi/\sqrt{\tilde{\epsilon}}a_0$, $\beta=\Delta\epsilon/4\tilde{\epsilon}$, $n_L=6\pi\chi^{(3)}/\tilde{\epsilon}$, $\eta=2\pi N_d/\tilde{\epsilon}$ and $\langle\ \rangle$ denotes averaging due to inhomogeneous broadening of the resonant atomic transition frequency ω_{ba}:

$$\langle p_{1,2}(x,t,\Delta\omega)\rangle=\int_{-\infty}^{\infty}p_{1,2}(x,t,\Delta\omega)g(\Delta\omega-\Delta\omega')d(\Delta\omega). \tag{2.7}$$

Here, $g(\Delta\omega'-\Delta\omega)$ is the probability distribution of *inhomogeneously* broadened energy levels of the resonant atoms, $\Delta\omega=\omega-\omega_{ba}$ is the detuning of the atomic transition frequency ω_{ba} from the incoming radiation frequency ω, and $\Delta\omega'$ is the detuning of the laser field frequency from the line center frequency ω_{ba}. For purely *homogeneous* broadening $g(\Delta\omega'-\Delta\omega)$ becomes simply a δ function and $\langle p_{1,2}\rangle=p_{1,2}$.

We now consider the underlying atomic Bloch equations for a periodic dielectric structure uniformly doped with resonant atoms. This involves a generalization of the derivation in ordinary vacuum found in most standard nonlinear optics textbooks [19]. The Heisenberg equation of motion for the 2×2 atomic density operator ρ is given by

$$i\hbar\frac{\partial\rho}{\partial t}=[H,\rho]+\{H,\Gamma\}. \tag{2.8}$$

Here the Hamiltonian $H=H_0+V(t)$ where H_0 denotes the atomic Hamiltonian, $V(t)$ denotes the interaction of the atom with the electromagnetic field, and Γ describes the damping processes due to radiative and nonradiative spontaneous emission, and other dephasing effects. We denote the lower atomic level by a and the upper level by b. In the electric-dipole approximation, $V(t)=-\mu E(t)$ where μ is the dipole moment and $E(t)$ is the applied electric field. From Eq. (2.8) the time evolution of the density matrix elements can be written as [19]

$$\frac{d}{dt}\rho_{ba}=-\left(i\omega_{ba}+\frac{1}{T_2}\right)\rho_{ba}+\frac{i}{\hbar}V_{ba}\rho_{\rm pop} \tag{2.9}$$

and

$$\frac{d}{dt}\rho_{\rm pop}=-\frac{\rho_{\rm pop}-\rho_{\rm pop}^0}{T_1}-\frac{2i}{\hbar}(V_{ba}\rho_{ab}-\rho_{ba}V_{ab}). \tag{2.10}$$

Here $\rho_{\rm pop}\equiv\rho_{bb}-\rho_{aa}$ describes the population difference of the atoms, which has an equilibrium value $\rho_{\rm pop}^0$ and ρ_{ba} is the atomic polarization. The effects of the matrix Γ have been included phenomenologically through the relaxation times T_1 and T_2 which describe the lifetime of the upper level and the dephasing time of the dipole moment, respectively. For a monochromatic applied field

$$V_{ba}=-\mu_{ba}(Ee^{-i\omega t}+E^*e^{i\omega t}), \tag{2.11}$$

a solution can be obtained in the form $\rho_{ba}=\sigma_{ba}e^{-i\omega t}$. In the rotating wave approximation, we neglect terms oscillating as $e^{\pm i2\omega t}$. In this case Eq. (2.10) becomes

$$\frac{d}{dt}\rho_{\rm pop}=-\frac{\rho_{\rm pop}-\rho_{\rm pop}^0}{T_1}-\frac{2i}{\hbar}(\mu_{ba}E\sigma_{ab}-\mu_{ab}E^*\sigma_{ba}). \tag{2.12}$$

Defining $\Delta\omega=\omega-\omega_{ba}$, $\sigma\equiv\sigma_{ba}$, $w=\rho_{bb}-\rho_{aa}$, $\mu\equiv\mu_{ba}$, and $p=\mu\sigma$ the optical Bloch equations become [19]

$$\frac{d}{dt}p=\left(i\Delta\omega-\frac{1}{T_2}\right)p-\frac{i}{\hbar}\mu^2Ew, \tag{2.13}$$

$$\frac{d}{dt}w=-\frac{w-w^{\rm eq}}{T_1}+\frac{2i}{\hbar}(Ep^*-E^*p). \tag{2.14}$$

In an extended Bragg scattering medium Eqs. (2.13) and (2.14) must be further simplified by separating the slow and fast varying spatial components of p, E, and w. A general Fourier expansion will lead to an infinite number of coupled equations. In the spirit of the SVEA we obtain a closed set of equations by keeping only the leading terms, namely,

$$p=p_1e^{ik_0x}+p_2e^{-ik_0x} \tag{2.15}$$

and

$$w = w_0 + w_1 e^{i2k_0 x} + w_1^* e^{-i2k_0 x}. \quad (2.16)$$

Inserting these expansions into the Bloch equations (2.13) and (2.14) we obtain the following coupled equations:

$$\frac{\partial p_1}{\partial t} = \left(i\Delta\omega - \frac{1}{T_2} \right) p_1 - i\frac{\mu^2}{\hbar}(E_1 w_0 + E_2 w_1), \quad (2.17)$$

$$\frac{\partial p_2}{\partial t} = \left(i\Delta\omega - \frac{1}{T_2} \right) p_2 - i\frac{\mu^2}{\hbar}(E_2 w_0 + E_1 w_1^*), \quad (2.18)$$

$$\frac{\partial w_0}{\partial t} = -\frac{(w_0 - w_{eq})}{T_1} + \frac{2i}{\hbar}(E_1 p_1^* + E_2 p_2^* - E_1^* p_1 - E_2^* p_2), \quad (2.19)$$

$$\frac{\partial w_1}{\partial t} = -\frac{w_1}{T_1} + \frac{2i}{\hbar}(E_1 p_2^* - E_2^* p_1), \quad (2.20)$$

where $\Delta\omega = 1 - \omega_{ba}$ is the detuning of the atomic transition frequency from the midgap frequency. Hereafter, all the frequencies are measured in units of ω_0. The times T_1 and T_2 are measured in units of ω_0^{-1}. Equations (2.5) and (2.6) and Eqs. (2.17)–(2.20) can be written in a compact form by introducing the 2×2 Pauli matrices (σ_x, σ_y, σ_y) and defining the two-component ''spinor'' fields $\Psi^\dagger = (E_1^*, E_2^*)$, $p^\dagger = (p_1^*, p_2^*)$, and $W^\dagger = (w_1^*, w_1)$:

$$i\frac{\partial \Psi}{\partial t} + i\sigma_z \frac{\partial \Psi}{\partial x} + \beta\sigma_x \Psi + n_L[3(\Psi^\dagger \Psi) - (\Psi^\dagger \sigma_z \Psi)\sigma_z]\Psi + \eta\langle p \rangle = 0, \quad (2.21)$$

$$\frac{\partial p}{\partial t} = \left(i\Delta\omega - \frac{1}{T_2} \right) p - i\frac{\mu^2}{\hbar} w_0 \Psi - i\frac{\mu^2}{2\hbar}[(W^\dagger \Psi)\varphi_1 - (W^\dagger \sigma_z \Psi)\varphi_2], \quad (2.22)$$

$$\frac{\partial w_0}{\partial t} = -\frac{(w_0 - w_{\rm eq})}{T_1} + \frac{2i}{\hbar}(p^\dagger \Psi - \Psi^\dagger p), \quad (2.23)$$

$$\frac{\partial W}{\partial t} = -\frac{W}{T_1} + \frac{i}{\hbar}\{[(p^\dagger \sigma_x \Psi) - (\Psi^\dagger \sigma_x p)]\varphi_1 - [(p^\dagger i\sigma_y \Psi) - (\Psi^\dagger i\sigma_y p)]\varphi_2\}. \quad (2.24)$$

Here, $\varphi_1^\dagger = (1,1)$ and $\varphi_2^\dagger = (1,-1)$. Equations (2.21)–(2.24) describe the Maxwell-Bloch equations for a uniformly doped periodic dielectric medium in the SVEA.

For reference purposes, we first consider the case of a harmonic medium in which $n_L = \eta = 0$. In this case, plane-wave solutions of the form $\Psi = \Phi e^{-i\Omega t + iqx}$ satisfy the dispersion relation

$$\Omega^2(q) = q^2 + \beta^2. \quad (2.25)$$

This gives two frequency branches $\Omega_\pm(q) = \pm\sqrt{q^2 + \beta^2}$ (see Fig. 1). The band edges occur when $q = 0$ at frequencies $\Omega_\pm = \pm\beta$. For frequencies $-\beta < \Omega < \beta$, q is purely imaginary and the field is exponentially attenuated within the medium. As a consequence, incident radiation of low intensity is completely reflected back. Outside the band gap, q is real,

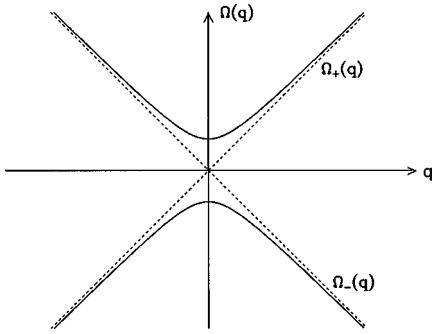

FIG. 1. The dispersion relation of the linear periodic structure. Plotted is the relation between Ω and q for a uniform medium ($\beta = 0$) (dotted line) and for a periodic grating in which the latter has a frequency gap of size 2β.

facilitating linear wave propagation within the medium. The eigenvectors of the upper and lower dispersion branches are given by

$$\Phi_\pm = \frac{1}{\sqrt{2\Omega_+(q)}} \begin{pmatrix} \sqrt{\Omega_+(q) \pm q} \\ \mp\sqrt{\Omega_+(q) \mp q} \end{pmatrix}. \quad (2.26)$$

Near the band edges ($q = 0$) we have $\Phi_+ = (1,-1)/\sqrt{2}$ and $\Phi_- = (1,1)/\sqrt{2}$ describing standing wave solutions, whereas when $q \to \infty$ then $\Phi_+ = (1,0)$ and $\Phi_- = (0,1)$, describing plane waves propagating to the right and left. It should be noted that here we have neglected the linear contribution to the dispersion relation arising from the two-level atoms. This is justified by the fact that we will treat the resonant atomic response exactly using the Bloch equations for a given density of dopant atoms. This treatment, however, considers the density of atoms, N_d, to be uniform. For a Poissonian distribution of atoms, there are fluctuations in the atomic density $\Delta N_d \simeq \sqrt{N_d}$. This in turn leads to random fluctuations in the linear dielectric susceptibility which may cause further scattering of the electromagnetic wave field. For the present treatment to be valid, we require that the root mean square fluctuations of the random linear susceptibility caused by density fluctuations of the resonant atoms should be small compared to the dielectric variation $\Delta\epsilon$ of the periodic, nonresonant PBG backbone. This places an upper limit on the allowed concentration of dopant atoms.

In general, the coupled Maxwell-Bloch equations (2.21)–(2.24) have to be solved numerically. Before proceeding to derive soliton solutions it is instructive to consider two special cases of these equations. As a first special case we set $w_1 = 0$. In this case, it is possible to obtain a set of coupled equations for E_1 and E_2 alone by eliminating the atomic variables. We may seek a solution of the form $E_{1,2}(x,t) = E_{1,2}(\zeta)e^{-i\delta t + ikx}$ and $p_{1,2}(x,t) = p_{1,2}(\zeta)e^{-i\delta t + ikx}$, where $\zeta = x - Vt$. Then Eqs. (2.21)–(2.23) can be written as (setting $w_1 = 0$)

$$i(1-V)\dot{E}_1 + (\delta - k)E_1 + \beta E_2 + n_L(|E_1|^2 + 2|E_2|^2)E_1 + \eta p_1 = 0, \quad (2.27)$$

$$-i(1+V)\dot{E}_2 + (\delta + k) + \beta E_1 + n_L(|E_2|^2 + 2|E_1|^2)E_2 + \eta p_2 = 0, \quad (2.28)$$

$$\dot{p}_1 = i\frac{\Delta}{V}p_1 - i\frac{\mu^2}{v\hbar}E_1 w_0, \tag{2.29}$$

$$\dot{p}_2 = i\frac{\Delta}{V}p_2 - i\frac{\mu^2}{v\hbar}E_2 w_0, \tag{2.30}$$

$$\dot{w}_0 = -\frac{2i}{\hbar V}(E_1 p_1^* + E_2 p_2^* - E_1^* p_1 - E_2^* p_2). \tag{2.31}$$

Here the dot represents the derivative with respect to the independent variable ζ, $\Delta = \omega - \omega_{ba}$, and $\omega = 1 + \delta$. We assume that the pulse duration τ_p is much shorter than the atomic relaxation times T_1 and T_2, so that no relaxation occurs for the duration of the pulse, in which case we set $T_1, T_2 \to \infty$. The validity of the slowly varying envelope function approximation nevertheless requires us to consider pulses for which $\tau_p \gg \omega_0^{-1}$. For $\omega_0 = 10^{15}\ \mathrm{s}^{-1}$, we require pulse widths of ten femtoseconds or more. Using p_1 and p_2 from Eqs. (2.27) and (2.28), the population inversion w_0 in Eq. (2.31) becomes

$$\dot{w}_0 = \frac{2}{\hbar V \eta}\frac{\partial}{\partial \zeta}[(1-V)|E_1|^2 - (1+V)|E_2|^2]. \tag{2.32}$$

This can be easily integrated to yield

$$w_0 = -1 + \frac{2}{\hbar V \eta}[(1-V)|E_1|^2 - (1+V)|E_2|^2], \tag{2.33}$$

where we have assumed that $[w_0(-\infty) = -1]$ all atoms are initially in their ground state. Having expressed the population inversion in terms of the electric field alone, we now substitute Eqs. (2.27) and (2.28) into Eqs. (2.29) and (2.30) and using Eq. (2.33) we obtain a set of coupled equations for E_1 and E_2 alone:

$$i\frac{\partial \hat{O}_1}{\partial \zeta} - \frac{\Delta}{V}\hat{O}_1 - \frac{\mu^2 \eta}{V\hbar}E_1 w_0 = 0, \tag{2.34}$$

$$i\frac{\partial \hat{O}_2}{\partial \zeta} - \frac{\Delta}{V}\hat{O}_2 - \frac{\mu^2 \eta}{V\hbar}E_2 w_0 = 0. \tag{2.35}$$

Here, the operators $\hat{O}_1$ and $\hat{O}_2$ are defined as

$$\hat{O}_1 = i(1-V)\dot{E}_1 + (\delta - k)E_1 + \beta E_2 + n_L(|E_1|^2 + 2|E_2|^2)E_1, \tag{2.36}$$

$$\hat{O}_2 = -i(1+V)\dot{E}_2 + (\delta + k)E_2 + \beta E_1 + n_L(|E_2|^2 + 2|E_1|^2)E_2. \tag{2.37}$$

The existence of an exact analytical solution to Eqs. (2.34) and (2.35) is not trivial. In general the solution to Eqs. (2.34) and (2.35) requires numerical methods. However, it is possible to obtain a simple effective Maxwell-Bloch equation by considering the case of an external laser field frequency which is tuned close to the photonic band edge. In this case we obtain analytical solutions describing some new types of solitary waves.

Steady-state solution to the Bloch equations

As a second special case of the general Maxwell-Bloch equations (2.21)–(2.24) we consider pulses that are longer than the relaxation times T_1 and T_2. In this case, the atomic system reaches its steady-state response more quickly than the time scale over which the laser field changes and consequently the Bloch equations can be adiabatically eliminated. We consider a steady laser field of the form $E_{1,2}, p_{1,2} \sim e^{-i\delta t}$, where δ is the frequency detuning from the photonic midgap. The steady-state response follows from setting the time derivative equal to zero in the Bloch equations (2.17)–(2.20). The quasistatic atomic polarization satisfies the equations

$$p_1 = i\frac{\mu^2}{\hbar\alpha}(E_1 w_0 + E_2 w_1) \tag{2.38}$$

and

$$p_2 = i\frac{\mu^2}{\hbar\alpha}(E_2 w_0 + E_1 w_1^*), \tag{2.39}$$

where $\alpha = i\Delta - 1/T_2$, and $\Delta = 1 + \delta - \omega_{ba}$ is the detuning of the laser frequency from the atomic transition frequency. Inserting Eqs. (2.38) and (2.39) into Eqs. (2.19) and (2.20) we get two coupled equations for w_0 and w_1:

$$w_0\left[\frac{1}{T_1} + \frac{2\mu^2\gamma}{\hbar^2}(|E_1|^2 + |E_2|^2)\right] = \frac{w_{\mathrm{eq}}}{T_1} - \frac{2\mu^2\gamma}{\hbar^2}[E_1 E_2^* w_1^* + E_1^* E_2 w_1], \tag{2.40}$$

$$w_1 = -\frac{2\mu^2\gamma}{\hbar^2}\frac{E_2^* E_1}{[1/T_1 + \gamma(|E_1|^2 + |E_2|^2) - i\Delta T_2(|E_1|^2 - |E_2|^2)]}w_0, \tag{2.41}$$

where $\gamma = 2T_2/(1 + \Delta^2 T_2^2)$. Equations (2.40) and (2.41) can be solved for w_0 and w_1. Inserting these results into Eqs. (2.38) and (2.39) yields a cumbersome expression for the nonlinear optical susceptibility χ, defined through the relation $P_{1,2} = \chi E_{1,2}$. In the absence of the Bragg scattering $w_1 = 0$, and we recover the textbook formula for χ [19].

When the field intensity is sufficiently small compared to the saturation intensity, the denominator can be expanded in powers of $|E_{1,2}|^2$. In the case that all atoms are in the ground state ($w_{\mathrm{eq}} = -1$) and $\Delta T_2 \gg 1$ the expansion for the polarization becomes

$$P_1 = -\frac{N_d \mu^2}{\hbar\Delta}\left[1 - \frac{4\mu^2 T_1}{\hbar^2 \Delta^2 T_2}(|E_1|^2 + 2|E_2|^2)\right]E_1. \tag{2.42}$$

P_2 is obtained from the above by interchanging the indices

1,2. This static limit describes a simple Kerr nonlinearity. However, this limit does not apply in the case of the high intensity, subpicosecond pulses which interact in a near resonant manner with the impurity atoms.

In contrast to the standard steady-state nonlinear susceptibility which we describe above, some entirely new effects are possible if the impurity atom transition lies deep inside of a complete three-dimensional PBG. In this case, the spontaneous emission rate $1/T_1$ is completely suppressed and the impurity atoms may exhibit coherent resonance dipole-dipole interaction (RDDI). This leads to very low threshold saturation of the individual atomic transition and a ''glass phase'' of the atomic dipoles [20]. The resulting nonlinear susceptibility differs dramatically from the above description. In particular, the imaginary part of the susceptibility can be strongly suppressed whereas the real part remains very large. However, in this paper we consider only the case of a low density of atoms tuned near the photonic band edge for which RDDI effects can be neglected.

III. APPROXIMATE SOLUTIONS TO THE MAXWELL-BLOCH EQUATIONS

Since it is difficult to obtain exact analytical solutions to the full Maxwell-Bloch equations described earlier, we consider soliton solutions in two special frequency regimes. In the first case, the resonant laser frequency and the atomic transition are both chosen to be far outside the PBG. In the second case, both are chosen to lie very near one of the photonic band edges.

Introducing the Fourier transformations,

$$\Psi(q,t)=\frac{1}{2\pi}\int dx e^{-iqx}\Psi(x,t), \tag{3.1}$$

$$p(q,t)=\frac{1}{2\pi}\int dx e^{-iqx}p(x,t), \tag{3.2}$$

we may rewrite Eq. (2.21) in momentum space as

$$[i\partial_t-q\sigma_z+\beta\sigma_x]\Psi(q,t)+F_{\rm nl}\{\Psi\}+\eta\langle p(q,t)\rangle=0. \tag{3.3}$$

Here, the nonlinear functional $F_{\rm nl}\{\Psi\}$ is given by

$$F_{\rm nl}\equiv\frac{n_L}{2}\int dq_1\int dq_2\{3\Psi^\dagger(q_1,t)\Psi(q_2,t)-[\Psi^\dagger(q_1,t)\sigma_z\Psi(q_2,t)]\sigma_z\Psi(q+q_1-q_2)\}. \tag{3.4}$$

The linear part of Eq. (3.3) can be diagonalized using the q-dependent unitary operator

$$S=\begin{pmatrix}\sin(\theta/2) & \cos(\theta/2)\\ \cos(\theta/2) & -\sin(\theta/2)\end{pmatrix}, \tag{3.5}$$

where $\tan(\theta)=\beta/q$. Introducing the new spinor field $\tilde{\Psi}(q,t)=S^\dagger(q)\Psi(q,t)$, Eq. (3.3) in the absence of nonlinear interaction ($n_L=0$) becomes

$$i\frac{\partial\tilde{\Psi}}{\partial t}=\sqrt{q^2+\beta^2}\sigma_z\tilde{\Psi}. \tag{3.6}$$

Near the photonic band edge ($q=0$), $S=(\sigma_x+\sigma_y)/\sqrt{2}$ and

$$\tilde{\Psi}=\frac{1}{\sqrt{2}}\begin{pmatrix}E_1+E_2\\ E_1-E_2\end{pmatrix} \tag{3.7}$$

describing standing wave solutions. Far from Bragg resonance ($q\to\infty$), $S=\sigma_x$ and

$$\tilde{\Psi}=\begin{pmatrix}E_2\\ E_1\end{pmatrix} \tag{3.8}$$

describing plane waves propagating to the left or right. These are the two limits for which we derive approximate solutions to the full nonlinear problem.

Frequency detuned far from Bragg resonance

When the laser frequency is detuned far from the Bragg resonance, $q/\beta\gg1$, then $\sqrt{q^2+\beta^2}\to q$, and the electromagnetic field is not strongly affected by the periodic structure. Accordingly, the results derived below are also valid for a uniform medium exhibiting a nonresonant Kerr response, doped with active atoms. Using the transformation S given by Eq. (3.8), Eq. (3.3) becomes

$$i\frac{\partial\tilde{\Psi}}{\partial t}+q\sigma_z\tilde{\Psi}+F_{\rm nl}\{\tilde{\Psi}\}+\eta\langle\tilde{p}\rangle=0. \tag{3.9}$$

Transforming back to coordinate space:

$$i\frac{\partial\tilde{\Psi}}{\partial t}-i\sigma_z\frac{\partial\tilde{\Psi}}{\partial x}+\frac{n_L}{2}[3(\tilde{\Psi}^\dagger\Psi)-(\tilde{\Psi}^\dagger\sigma_z\tilde{\Psi})\sigma_z]\tilde{\Psi}+\eta\langle\tilde{p}\rangle=0. \tag{3.10}$$

The corresponding Bloch equations are

$$\frac{\partial\tilde{p}}{\partial t}=i\Delta\omega\tilde{p}-i\frac{\mu^2}{\hbar}\tilde{\Psi}w_0-i\frac{\mu^2}{2\hbar}[(\tilde{W}^\dagger\tilde{\Psi})\varphi_1-(\tilde{W}^\dagger\sigma_z\tilde{\Psi})\varphi_2], \tag{3.11}$$

$$\frac{\partial w_0}{\partial t}=\frac{2i}{\hbar}(\tilde{p}^\dagger\tilde{\Psi}-\tilde{\Psi}^\dagger\tilde{p}), \tag{3.12}$$

and

$$\frac{\partial\tilde{W}}{\partial t}=\frac{i}{\hbar}\{[(\tilde{p}^\dagger\sigma_x\tilde{\Psi})-(\tilde{\Psi}^\dagger\sigma_x\tilde{p})]\varphi_1-[(\tilde{p}^\dagger i\sigma_y\tilde{\Psi})-(\tilde{\Psi}^\dagger i\sigma_y\tilde{p})]\varphi_2\}. \tag{3.13}$$

Here, $\tilde{p}=S^\dagger p$ and $\tilde{W}=S^\dagger W$. For illustrative purposes we consider an optical pulse moving to the right (upper branch of the dispersion), $\tilde{\Psi}_+^\dagger=(0,E_1^*)$. In general, the $\tilde{W}$ terms arise from Bragg scattering of the incident pulse. Far away from the band gap, the backscattered field is negligible and accordingly we seek a solution for which $\tilde{W}=0$. Introducing

the notation $w \equiv w_0$, $p \equiv p_1$, and $E \equiv E_1$, we obtain the one-component Maxwell-Bloch equations:

$$i\frac{\partial E}{\partial t} + i\frac{\partial E}{\partial x} + n_L|E|^2E + \eta\langle p\rangle = 0, \tag{3.14}$$

$$\frac{\partial p}{\partial t} = i\Delta\omega p - i\frac{\mu^2}{\hbar}Ew, \tag{3.15}$$

$$\frac{\partial w}{\partial t} = \frac{2i}{\hbar}(p^*E - E^*p). \tag{3.16}$$

When the nonlinear effect (Kerr response) of the host medium is negligible ($n_L = 0$), it is straightforward to recapture the usual McCall and Hahn (SIT) soliton. In the more general case ($n_L \neq 0$) it is necessary to include phase modulation $\phi(\zeta)$ and consider a trial solution of the form $E(x,t) = \varepsilon(\zeta)e^{-i\delta t + ikx + i\phi(\zeta)}$ and $p(x,t) = [u(\zeta) + iv(\zeta)]e^{-i\delta t + ikx + i\phi(\zeta)}$, where $\zeta = t - x/V$, V is the velocity of the solitary wave measured in units of the average speed of light in the uniform medium $c/\sqrt{\tilde{\epsilon}}$, δ is the detuning from the midgap, and k is a yet to be determined wave vector shift. Separating the real and imaginary components we obtain

$$-\tau\dot{\varepsilon} + \eta\langle v\rangle = 0, \tag{3.17}$$

$$\tau\varepsilon\dot{\phi} + (\delta - k)\varepsilon + n_L\varepsilon^3 + \eta\langle u\rangle = 0, \tag{3.18}$$

$$\dot{u} - \dot{\phi}v = -\delta_a v, \tag{3.19}$$

$$\dot{v} + \dot{\phi}u = \delta_a u - \frac{\mu^2}{\hbar}\varepsilon w, \tag{3.20}$$

$$\dot{w} = \frac{4}{\hbar}\varepsilon v, \tag{3.21}$$

where $\tau = 1/V - 1$ and $\delta_a = \omega - \omega_{ba}$ is the detuning of the atomic transition frequency ω_{ba} from the field frequency $\omega = 1 + \delta$. The angular brackets $\langle\ \rangle$ denote an average over the inhomogeneously broadened atomic spectrum as defined by Eq. (2.7). In this paper we derive an analytic solution in the sharp-line limit $\langle u\rangle = u$ and $\langle v\rangle = v$. Soliton solutions in the presence of inhomogeneous line broadening require numerical methods. Using v from Eq. (3.17) in Eq. (3.21), the population inversion can be expressed as

$$w = -1 + \frac{2\tau}{\hbar\eta}\varepsilon^2. \tag{3.22}$$

Using Eqs. (3.17) and (3.18) we may express the atomic polarization variables in terms of the field variables ε and ϕ. In this case Eq. (3.19) becomes

$$\tau\ddot{\varepsilon} + (\delta_a - \dot{\phi})[\tau\dot{\phi}\varepsilon + (\delta - k)\varepsilon + n_L\varepsilon^3] + \frac{\eta\mu^2}{\hbar}\varepsilon w = 0, \tag{3.23}$$

and Eq. (3.20) becomes

$$\tau\varepsilon\ddot{\phi} + 2\tau\dot{\varepsilon}\dot{\phi} - \dot{\varepsilon}(k - \delta + \tau\delta_a) + 3n_L\varepsilon^2\dot{\varepsilon} = 0. \tag{3.24}$$

Multiplying Eq. (3.24) by ε and then integrating once yields

$$\dot{\phi} = -\frac{3n_L}{4\tau}\varepsilon^2 + \frac{c_1}{\tau\varepsilon^2} + \frac{1}{2}(k - \delta + \tau\delta_a), \tag{3.25}$$

where c_1 is a constant of integration. $\partial\phi/\partial t$ describes the instantaneous frequency shift from the average frequency. This frequency shift (chirp) arises purely from the nonlinear interactions. When $n_L = 0$ and $c_1 = 0$ we require that this phase modulation vanishes. This determines the wave vector shift $k = \delta - \tau\delta_a$. In the case when $n_L = 0$, the single-pulse soliton discovered by McCall and Hahn follows immediately from the above equations by setting $c_1 = 0$. For $c_1 \neq 0$, Eqs. (3.25) and (3.23) describe pulse train solutions [21–23], which have been observed experimentally [24]. To illustrate the nature of these solutions we consider the on resonance case $\delta_a = 0$ and neglect the host nonlinear Kerr coefficient $n_L = 0$. Inserting Eq. (3.25) into Eq. (3.23) we obtain an equation for ε only,

$$\ddot{\varepsilon} - \gamma_1\varepsilon^{-3} - \gamma_2\varepsilon + \gamma_3\varepsilon^3 = 0, \tag{3.26}$$

where $\gamma_1 = c_1^2/\tau^2$, $\gamma_2 = \eta\mu^2/\hbar\tau$, and $\gamma_3 = 2\mu^2/\hbar^2$. Equation (3.26) can be integrated once to yield

$$(\dot{\varepsilon})^2 + c_2 + \gamma_1\varepsilon^{-2} - \gamma_2\varepsilon^2 + \frac{\gamma_3}{2}\varepsilon^4 = 0, \tag{3.27}$$

where c_2 is another constant of integration. Defining $S = \varepsilon^2$ Eq. (3.27) can be reexpressed as

$$\frac{(\dot{S})^2}{4} + \gamma_1 + c_2 S - \gamma_2 S^2 + \frac{\gamma_3}{2}S^3 = 0. \tag{3.28}$$

Equation (3.28) is of the form $(\dot{S})^2 + U(S) = 0$, and is amenable to solution by means of a mechanical analogy. It describes the motion of a classical particle moving in a potential $U(S)$. Consider first the case when there is no chirping: $c_1 = c_2 = 0$. In Fig. 2(a) we plot the potential $U(S)$. The zeros of the potential can easily be found as $S = 0$ and $S = 2\gamma_2/\gamma_3$. The soliton solution corresponds to the case when the particle is released at $S = 2\gamma_2/\gamma_3$ and comes to rest at $S = 0$, resulting in a single-pulse solution. On the other hand, when $c_{1,2} \neq 0$ we obtain a class of extended solutions, determined by the zeros of the potential. One such solution is depicted in Fig. 2(b) where the particle is released at $S = S_1$ and oscillates between S_1 and S_2. The negative root is eliminated on physical grounds since $S = \varepsilon^2 > 0$. Equation (3.28) can be further integrated to yield

$$\int_{S_0}^{S}\frac{dS}{\sqrt{\gamma_2 S^2 - \gamma_3 S^3/2 - 2c_2 S - \gamma_1}} = \int_{S_0}^{S}\frac{dS}{\sqrt{P_3(S)}} = 2\zeta. \tag{3.29}$$

The integral of Eq. (3.29) can have a class of solution related to the elliptic functions, and the solution depends on the roots of $P_3(S)$ [25]. To obtain a physical solution we must

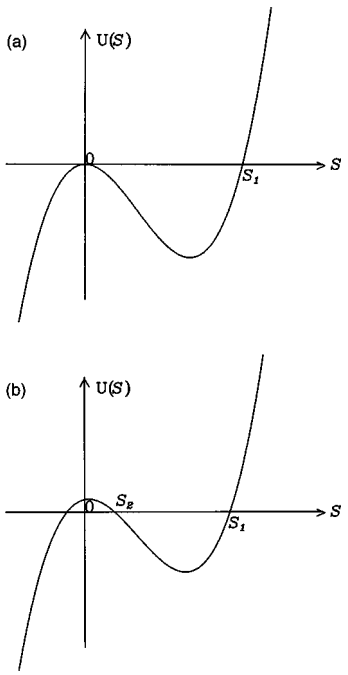

FIG. 2. Plotted is the potential $U(S)$ in which the classical particle moves for $n_L=0$. (a) The potential in the case when $c_{1,2}=0$. In this case the soliton solution corresponds to a particle being released from $S=S_1$ and coming to rest at $S=0$ which results in single-pulse hyperbolic secant solution. (b) The potential when $c_{1,2}\neq 0$. Here the particle is released at $S=S_1$ goes to $S=S_2$ but returns back to S_1. Consequently the particle oscillates between S_1 and S_2 resulting in a periodic pulse train.

have at least two positive real roots S_1 and S_2. Similar solutions can also be found in the case when $n_L\neq 0$ [17].

We restrict our attention here to the nature of single-pulse solitons for which $c_1=0$. Using Eq. (3.25) in Eq. (3.23) we obtain

$$\ddot{\varepsilon}=(\alpha_1\varepsilon-\alpha_2\varepsilon^3-\alpha_3\varepsilon^5), \tag{3.30}$$

where $\alpha_1=-\delta_a^2+\eta\mu^2/\tau$, $\alpha_2=\delta_a n_L/\tau+2\mu^2/\hbar^2$, and $\alpha_3=3n_L^2/16\tau^2$. Now Eq. (3.30) can be rewritten in the form

$$\ddot{\varepsilon}=-\frac{\partial U}{\partial\varepsilon}, \tag{3.31}$$

with $U=-\alpha_1\varepsilon^2/2+\alpha_2\varepsilon^4/4+\alpha_3\varepsilon^6/6$. Equation (3.31) describes a classical particle moving in a potential U. In Fig. 3 we plot the potential $U(\varepsilon)$. The solitary wave solution corresponds to the particle starting at point $\varepsilon=\varepsilon_0$ and stopping at the hill where $\varepsilon=0$. Accordingly, the amplitude ε_0 corresponds to the zeros of $U(\varepsilon)$. The physically admissible solution is

$$\varepsilon_0^2=\frac{-\alpha_2/4+\sqrt{(\alpha_{2/4})^2+\alpha_1\alpha_3/3}}{\alpha_3/3}. \tag{3.32}$$

Equation (3.30) is known as the nonlinear cubic-quintic Schrödinger equation and has an exact analytical solution given by [26,27]

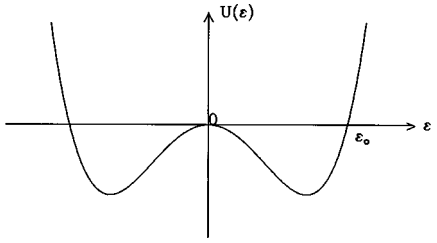

FIG. 3. Shown is the potential $U(\varepsilon)$ for the case when $c_1=0$ and $n_L\neq 0$. The soliton solution corresponds to the particle being released from $\varepsilon=\varepsilon_0$ and coming to rest at the hill where $\varepsilon=0$.

$$\varepsilon(\zeta)=\varepsilon_0\frac{\operatorname{sech}(a\zeta)}{\sqrt{1+b^2\tanh^2(a\zeta)}}. \tag{3.33}$$

The relation between the pulse width, velocity, and the density remains the same as given in the McCall-Hahn solution:

$$\tau(a^2+\delta_a^2)=\frac{\eta\mu^2}{\hbar}. \tag{3.34}$$

On the other hand,

$$b=\frac{n_L\varepsilon_0^2}{4\tau a}. \tag{3.35}$$

Finally, the phase angle ϕ is obtained from Eq. (3.25):

$$\phi(\zeta)=\phi_0-3\arctan[b\ \tanh(a\zeta)]. \tag{3.36}$$

Before we discuss the case when $n_L\neq 0$ we briefly review the McCall-Hahn solution. When $n_L=0$ and $c_3=0$, Eq. (3.30) reduces to the nonlinear Schrödinger equation. This has the well known hyperbolic-secant solution:

$$\varepsilon(\zeta)=\frac{a\hbar}{\mu}\operatorname{sech}(a\zeta). \tag{3.37}$$

The relation between the pulse width and the velocity is given by Eq. (3.34). The polarization components u and v have the well known forms [28]

$$v=-\frac{a^2\mu}{(a^2+\delta_a^2)}\operatorname{sech}(a\zeta)\tanh(a\zeta) \tag{3.38}$$

and

$$u=-\frac{a^2\mu\delta_a}{(a^2+\delta_a^2)}\operatorname{sech}(a\zeta). \tag{3.39}$$

The atomic population inversion is given as

$$w=-1+\frac{2a^2}{(a^2+\delta_a^2)}\operatorname{sech}(a\zeta). \tag{3.40}$$

The solution obtained for a homogeneously broadened medium can easily be extended to an inhomogeneously broadened medium. This is obtained from the factorization ansatz $v(\delta_a,\zeta)=f(\delta_a)v(0,\zeta)$ which yields a self-consistent solution of the Maxwell-Bloch equations. In this case, Eq. (3.34) is replaced by

$$a^2\tau=\int_{-\infty}^{+\infty} d\delta_a g(\delta_a'-\delta_a) f(\delta_a), \tag{3.41}$$

where $f(\delta_a)=a^2/(a^2+\delta_a^2)$ and $g(\delta_a'-\delta_a)$ is the inhomogeneous distribution function as defined previously.

In the absence of Kerr nonlinearity of the host material ($n_L=0$), the atomic Bloch equations can be written in a compact form by defining the Bloch vector $\vec{R}=(2u/\mu,2v/\mu,w)$ and $\vec{\Omega}=(2\mu\varepsilon/\hbar,0,\delta_a)$:

$$\frac{d\vec{R}}{dt}=\vec{\Omega}\times\vec{R}. \tag{3.42}$$

For instance, when $\delta_a=0$, then $u=0$ and the Bloch vector lies in the (v,w) plane. As the optical pulse goes through the medium the atoms are excited and then return to their ground state. This corresponds to a 2π rotation of the Bloch vector as well as a 2π pulse area. However, when $n_L\neq 0$, ϕ enters in the Bloch equations and Eq. (3.42) is replaced by

$$\frac{d\vec{R}}{dt}=\vec{\Omega}\times\vec{R}+\frac{d\phi}{dt}\gamma\vec{R}, \tag{3.43}$$

where the 3×3 matrix γ is given as

$$\gamma=\begin{pmatrix} 0 & 1 & 0 \\ -1 & 0 & 0 \\ 0 & 0 & 0 \end{pmatrix}. \tag{3.44}$$

The passage of the optical soliton pulse leads to polarization components u and v of the form

$$v=-\frac{\tau\varepsilon_0 a(1+b^2)}{\eta}\frac{\mathrm{sech}(a\zeta)\tanh(a\zeta)}{[1+b^2\tanh^2(a\zeta)]^{3/2}}, \tag{3.45}$$

$$u=-\frac{\tau\delta_a}{\eta}\varepsilon_0\frac{\mathrm{sech}(a\zeta)}{[1+b^2\tanh^2(a\zeta)]^{1/2}} -\frac{\tau b a}{\eta}\varepsilon_0\frac{\mathrm{sech}^3(a\zeta)}{[1+b^2\tanh^2(a\zeta)]^{3/2}}, \tag{3.46}$$

and the population inversion takes the form

$$w=-1+\frac{2\tau\varepsilon_0^2}{\hbar\eta}\frac{\mathrm{sech}(a\zeta)}{1+b^2\tanh^2(a\zeta)}. \tag{3.47}$$

The generalization of the SIT-Kerr solution to include inhomogeneous line broadening effects requires numerical methods since the factorization ansatz of McCall and Hahn is no longer applicable.

The inclusion of the nonresonant Kerr nonlinearity in a medium uniformly doped with two-level atoms has also been considered by Matulic and Eberly [17]. They found an approximate result by treating the Kerr coefficient perturbatively. Their result (valid when $b\ll 1$) can be recaptured by setting the denominator term in Eqs. (3.33), (3.45), and (3.46) to unity. In this case, the phase modulation simply becomes $\phi\sim d\ \tanh(a\zeta)$. Here, we obtain an exact analytical solution valid for the entire range of parameter values. From Eq. (3.34) we can see that the relation between the pulse width and velocity is not affected by the Kerr nonlinearity and is the same as in the case of the regular (SIT) solution. However, as we can see from Eq. (3.32) the amplitude now also depends on the Kerr coefficient, the atomic detuning δ_a, and the dopant density N_d. This is very different than the regular McCall and Hahn (SIT) soliton where $A^2=\hbar^2a^2/\mu^2$. In the limit when $n_L\to 0$, we recover the usual SIT soliton solution. In general, the Kerr coefficient has a significant effect on the soliton solution. The envelope function is not a simple hyperbolic secant type of function and the pulse width is not purely determined by the parameter a when b becomes larger than unity.

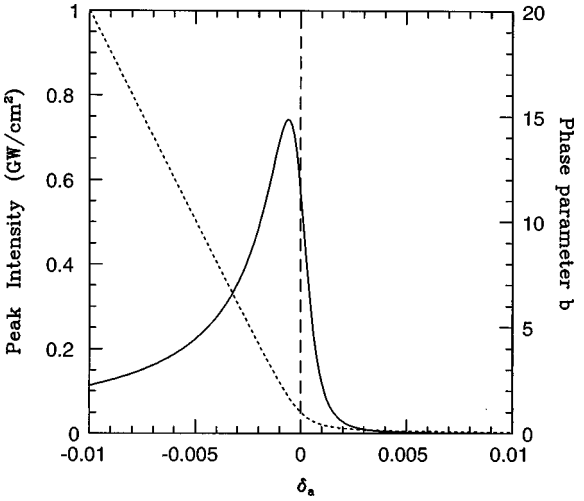

FIG. 4. Plotted is the peak intensity (solid line) and the phase parameter b (dotted line) of the soliton for a fixed value $a=10^{-3}$ as a function of the detuning frequency $\delta_a=\omega-\omega_{ba}$. The other material parameters are chosen as $\mu=10^{-19}$ (esu), $n_L=10^{-10}$ (esu), and $\eta=10^{18}$ cm^{-3}.

We now consider a numerical example to explore the parameter space of the analytical solution. We consider the parameters $\mu=10^{-19}$ (esu), $n_L=10^{-10}$ (esu), and $\eta=10^{18}$ cm^{-3}. We assume that $a=10^{-3}$ (which in our notation correspond to a pulse width of 1 ps), and $\omega_0\simeq 10^{15}$ s^{-1} ($\lambda=1.55$ μm). In Fig. 4 the peak pulse intensity $I=c\sqrt{\tilde{\epsilon}}|E|^2/2\pi$ and the phase parameter b are plotted in terms of the atomic detuning frequency $\delta_a=\omega-\omega_{ba}$. As can be seen, there is a significant difference when the field frequency ω is detuned above versus below the atomic transition frequency ω_{ba}.

For the on resonance case ($\delta_a=0$), the peak intensity $I=0.4$ GW/cm^2 and $b=1.0$. When $\delta_a=0.005$ the peak intensity becomes 1.7 MW/cm^2 with $b=0.1$, whereas when $\delta_a=-0.005$ we have $I=0.17$ GW/cm^2 and $b=10$. The parameter b has an important effect on the overall pulse width. When $b\ll 1$, the soliton profile is given by a simple hyperbolic secant function with a pulse width of $1/a$. On the other hand, when $b\gg 1$ there are significant deviations from the simple hyperbolic-secant function and the pulse width becomes narrower. This effect is shown in Fig. 5, where the pulse intensity on resonance (solid line) is contrasted with that for $\delta_a=-0.005$. In the latter case, the pulse width narrows significantly. If we neglect the Kerr nonlinearity, then for the same parameters the peak intensity is about $I=140$ GW/cm^2.

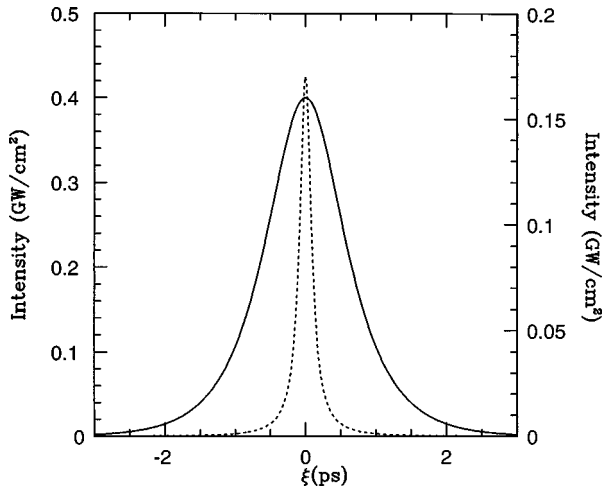

FIG. 5. Plotted is the intensity profile of the soliton solution for $\delta_a=0$ (solid line) (left scale) and for $\delta_a=-0.005$ (dotted line) (right scale). The material parameters are chosen as $\mu=10^{-19}$ (esu), $n_L=10^{-10}$ (esu), and $\eta=10^{18}$ cm^{-3}.

To further elucidate the nature of this solution, we plot in Fig. 6 the peak intensity as a function of the pulse width parameter a for $\delta_a=0$, with all the other parameters being fixed. In this case the amplitude takes the form

$$\varepsilon_0^2=\frac{8\eta^2\mu^6}{n_L^2\hbar^4a^4}\left(-1+\sqrt{1+\frac{a^6n_L^2\hbar^6}{4\eta^2\mu^8}}\right). \tag{3.48}$$

The intensity increases starting from long pulses down to about 5 ps but starts to decrease sharply as the pulse width becomes shorter than 5 ps. In the McCall-Hahn (SIT) soliton, the intensity continues to increase very rapidly as the pulse width becomes on the order of picoseconds. In order to create a soliton in the coherent interaction regime, one must use picosecond or subpicosecond pulses which in turn require large powers. Using the combined effect of the nonlinear Kerr response and two-level atoms, solitons can be realized experimentally using lower intensity fields. The results presented above have assumed that the Kerr coefficient is positive. The solution for a negative Kerr coefficient can be simply obtained by mirror reflecting the plot in Fig. 4 with respect to $\delta_a=0$.

We note finally that the solution described above is similar to that obtained by Bowden *et al.* [29], including the effect of the near dipole-dipole (NDD) interaction between atoms at high densities into the Bloch equations, but with $n_L=0$. The resulting envelope function ε satisfies a nonlinear cubic-quintic Schrödinger equation given by Eq. (3.30) and is accompanied by a similar phase modulation function ϕ.

IV. SELF-INDUCED TRANSPARENCY NEAR A PHOTONIC BAND EDGE

As a second limiting case, we consider the resonant interaction of an optical pulse with two-level atoms when Bragg scattering of the electromagnetic wave is dominant. The photonic band edges occur at $q=0$. Consequently the band-edge behavior may be described by expanding the dispersion relation $\Omega(q)$ for small q $(q/\beta\ll 1)$:

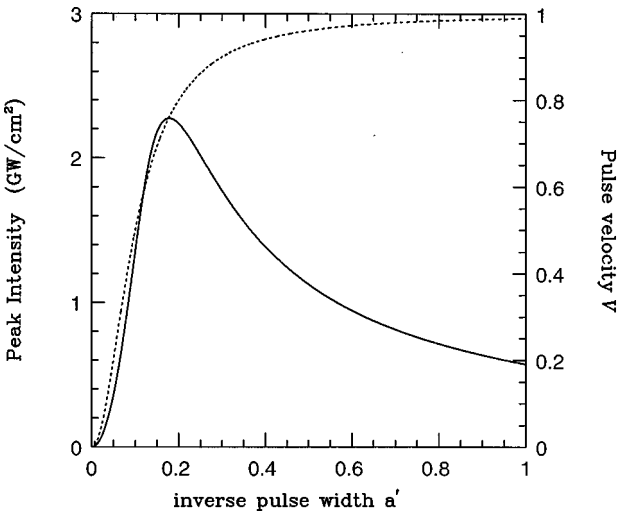

FIG. 6. The peak intensity (solid line) and pulse velocity (dotted line) (measured in units of the average speed of light $c/\sqrt{\tilde{\epsilon}}$ in the medium) for $\delta_a=0$ are plotted as a function of $a'=10^3a$, where a is the inverse pulse duration [see Eq. (3.33)] measured in units of ω_0. The other material parameters are chosen as $\mu=10^{-19}$ (esu), $n_L=10^{-10}$ (esu), and $\eta=10^{18}$ cm^{-3}.

$$\Omega(q)=\left(\Omega_0+\frac{\Omega''}{2}q^2+\cdots\right), \tag{4.1}$$

where $\Omega_0=\Omega(0)=\beta$ and $\Omega''=(\partial^2\Omega/\partial q^2)|_{q=0}=1/\beta$. Inserting the expansion (4.1) into Eq. (3.3) we obtain

$$i\frac{\partial\tilde{\Psi}}{\partial t}+\left(\Omega_0+\frac{q^2}{2}\Omega''\right)\sigma_z\tilde{\Psi}+\frac{n_L}{2}\{3(\tilde{\Psi}^\dagger\tilde{\Psi})-(\tilde{\Psi}^\dagger\sigma_x\tilde{\Psi})\sigma_x\}\tilde{\Psi}+\eta\langle\tilde{p}\rangle=0, \tag{4.2}$$

where $\tilde{\Psi}(q,t)=S(0)\Psi(q,t)$ and $\tilde{p}=S(0)p$. Within this approximation we replaced $S(q)$ by $S(0)$, where $S(0)$ is defined in the preceding section. This approximation is valid provided that the soliton spectrum is centered sharply around $q=0$. This means that in coordinate space the soliton envelope function extends over many lattice constants. Transforming Eq. (4.2) back to coordinate space we obtain the following effective nonlinear wave equation:

$$i\frac{\partial\tilde{\Psi}}{\partial t}-\frac{\Omega''}{2}\sigma_z\frac{\partial^2\tilde{\Psi}}{\partial x^2}+\beta\sigma_z\tilde{\Psi}+\frac{n_L}{2}\{3(\tilde{\Psi}^\dagger\tilde{\Psi})-(\tilde{\Psi}^\dagger\sigma_x\tilde{\Psi})\sigma_x\}\tilde{\Psi}+\eta\langle\tilde{p}\rangle=0. \tag{4.3}$$

Applying the same transformation to the atomic Bloch equations yields

$$\frac{\partial\tilde{p}}{\partial t}=i\Delta\omega\tilde{p}-i\frac{\mu^2}{\hbar}\tilde{\Psi}w_0-i\frac{\mu^2}{\sqrt{2}\hbar}[(\tilde{W}^\dagger\tilde{\Psi})\phi_1-(\tilde{W}^\dagger\sigma_x\tilde{\Psi})\phi_2], \tag{4.4}$$

$$\frac{\partial w_0}{\partial t}=\frac{2i}{\hbar}(\tilde{p}^\dagger\tilde{\Psi}-\tilde{\Psi}^\dagger\tilde{p}), \tag{4.5}$$

$$\frac{\partial \tilde{W}}{\partial t}=\frac{2i}{\sqrt{2}\hbar}\{[(\tilde{p}^{\dagger}\sigma_z\tilde{\Psi})-(\tilde{\Psi}^{\dagger}\sigma_z\tilde{p})]\phi_1+[(\tilde{p}^{\dagger}i\sigma_y\tilde{\Psi})-(\tilde{\Psi}^{\dagger}i\sigma_y\tilde{p})]\phi_2\}. \tag{4.6}$$

Here $\phi_1^{\dagger}=(1,0)$, $\phi_2^{\dagger}=(0,1)$, and $\tilde{W}=S(0)W$.

We may consider two specific solutions $\tilde{\Psi}^{\dagger}=(\tilde{E}_1,0)$ and $\tilde{\Psi}^{\dagger}=(0,\tilde{E}_2)$ which correspond to the lower band edge and upper band edge, respectively. Near the upper band edge, the ansatz $\tilde{\Psi}^{\dagger}=(0,\tilde{E}_2)$ and $\tilde{p}^{\dagger}=(0,\tilde{p}_2)$ reduces Eq. (4.3) to

$$i\frac{\partial E}{\partial t}+\frac{\Omega''}{2}\frac{\partial^2 E}{\partial x^2}-\beta E+i\Gamma E+3n_L|E|^2E+\eta\langle p\rangle=0. \tag{4.7}$$

Here, $\tilde{E}_2=(E_1-E_2)/\sqrt{2}=\sqrt{2}E_1$, $\tilde{p}_2=\sqrt{2}p_1$, and we have renamed $E_1=E$, $p_1=p$. Also $\tilde{W}^{\dagger}=(\sqrt{2}w_1,0)$. In order to make our model more realistic, we have also added linear losses ($\Gamma>0$) or gain ($\Gamma<0$). In order to extract analytical results we neglect the effects of inhomogeneous line broadening in what follows and set $\langle p\rangle=p$. Later we will discuss a special case for which inhomogeneous broadening can be treated analytically. Inserting the same ansatz into the Bloch equations (4.4)–(4.6) yields

$$\frac{\partial p}{\partial t}=\left(i\Delta\omega-\frac{1}{T_2}\right)p-i\frac{\mu^2}{\hbar}E(w_0-w_1), \tag{4.8}$$

$$\frac{\partial w_0}{\partial t}=\frac{4i}{\hbar}(p^*E-pE^*), \tag{4.9}$$

$$\frac{\partial w_1}{\partial t}=\frac{2i}{\hbar}(pE^*-p^*E). \tag{4.10}$$

Here we have included the effects of the dipole-dephasing time T_2, which may arise from atom-atom collisions or the interaction of atoms with lattice vibrations of the host material. The time scale for T_2 in rare-earth doped glass fibers is in the range of nanoseconds to femtoseconds. However, in most cases cooling down the solid increases T_2. The upper level lifetime T_1 is neglected, since for atoms doped in a solid, T_1 is on the order of ms to μs. For instance, for an erbium doped glass the lifetime of the transition $^4I_{13/2}\rightarrow{}^4I_{15/2}$ corresponding to 1.5 μm is about 10 ms and the dipole-dephasing time is on the order of one picosecond [30,31]. Since we are dealing with nanosecond to subpicosecond pulses we may safely take the limit $T_1\rightarrow\infty$. We will show in what follows that under certain conditions dipole dephasing and linear gain may offset each other, leading to a soliton solution. As expected, near the band edge we have a contribution from the W term, since both the forward and backward fields contribute almost equally to the effective field. Equations (4.8)–(4.10) can be reduced to the standard form of the Maxwell-Bloch equations by defining $\bar{w}=w_0-w_1$:

$$\frac{\partial p}{\partial t}=\left(i\Delta\omega-\frac{1}{T_2}\right)p-i\frac{\mu^2}{\hbar}E\bar{w}, \tag{4.11}$$

$$\frac{\partial \bar{w}}{\partial t}=\frac{6i}{\hbar}(p^*E-pE^*). \tag{4.12}$$

As before, we seek a general solution of the form $E(x,t)=\varepsilon(\zeta)e^{-i(\beta-\delta)t+ikx+i\phi(\zeta)}$ and $p(x,t)=(u+iv)e^{-i(\beta-\delta)t+ikx+i\phi(\zeta)}$ where $\zeta=t-x/V$ and V is the velocity of the solitary wave. Inserting this ansatz into the Maxwell-Bloch equations yields

$$\tau\varepsilon\dot{\phi}+\frac{\Omega''}{2V^2}\ddot{\varepsilon}-\frac{\Omega''}{2V^2}\varepsilon\dot{\phi}^2-\alpha\varepsilon+3n_L\varepsilon^3+\eta u=0, \tag{4.13}$$

$$-\tau\dot{\varepsilon}+\frac{\Omega''}{V^2}\dot{\varepsilon}\dot{\phi}+\frac{\Omega''}{2V^2}\varepsilon\ddot{\phi}+\Gamma\varepsilon+\eta v=0, \tag{4.14}$$

$$\dot{u}-\dot{\phi}v=-\delta_a v-\frac{u}{T_2}, \tag{4.15}$$

$$\dot{v}+\dot{\phi}u=\delta_a u-\frac{\mu^2}{\hbar}\varepsilon\bar{w}-\frac{v}{T_2}, \tag{4.16}$$

$$\dot{\bar{w}}=\frac{12}{\hbar}\varepsilon v. \tag{4.17}$$

Here, $\tau=\Omega''k/V-1$, $\alpha=(\delta+k^2\Omega''/2)$, and δ is defined as the detuning from the upper band edge. Since our formulation is restricted to near band-edge behavior it is assumed that $|\delta|\ll 1$ ($\delta>0$ inside the gap, $\delta<0$ outside the gap). The total field frequency is given as $\omega=1+\beta-\delta$ and $\delta_a=\omega-\omega_{ba}$ is the detuning of the average laser frequency from the atomic transition frequency.

First we consider the case of no losses, $\Gamma=0$, $T_2\rightarrow\infty$, in the sharp-line limit. Using v from Eq. (4.14) the population inversion can be integrated once to give

$$\bar{w}=-1+\frac{6\varepsilon^2}{\hbar\eta}\left(\tau-\frac{\Omega''}{V^2}\dot{\phi}\right), \tag{4.18}$$

where we have chosen $w(-\infty)=-1$. That is to say, all atoms are initially in their ground state. Our band-edge approximation entails the assumptions that the envelope function is extended over many lattice constants ($a\ll 1$), and that the soliton velocity $V\ll 1$. Furthermore, we make the assumption that the phase $\phi\ll 1$. In the spirit of the SVEA, we neglect the $(\dot{\phi})^2$ term in Eq. (4.13) and likewise the higher derivative terms in Eq. (4.14). We then insert the trial solution for the envelope function $\varepsilon=A\ \mathrm{sech}(a\zeta)$ and the phase $\phi=d\ \tanh(a\zeta)$ into Eqs. (4.13) and (4.14) and solve for u and v. This yields

$$v=-\frac{\tau A a}{\eta}\,\mathrm{sech}(a\zeta)\tanh(a\zeta), \tag{4.19}$$

$$u=-\frac{A}{\eta}\left(\frac{\Omega''a^2}{2V^2}-\alpha\right)\mathrm{sech}(a\zeta)-\frac{A}{\eta}\left(3n_LA^2+\tau da-\frac{\Omega''a^2}{V^2}\right)\mathrm{sech}^3(a\zeta). \tag{4.20}$$

Using these expressions in Eqs. (4.15) and (4.16) and keeping only terms up to a^2 and ad, we obtain the following relations:

$$\frac{\Omega'' a^2}{2V^2} = \alpha + \tau\delta_a , \tag{4.21}$$

$$n_L A^2 = \frac{\Omega'' a^2}{3V^2} - \frac{4}{9}\tau d a, \tag{4.22}$$

$$\tau(a^2 + \delta_a^2) = \frac{\mu^2 \eta}{\hbar}, \tag{4.23}$$

$$\frac{3\mu^2}{\hbar^2} A^2 = a^2 + \frac{2}{3}\delta_a d a. \tag{4.24}$$

In what follows we consider two separate physical situations. In the first case the Kerr effect is significant ($n_L \neq 0$) and in the second case $n_L = 0$.

A. Solitary waves in a nonlinear Bragg grating doped with resonance two-level atoms

The relative importance of the nonresonant Kerr effect is determined by the magnitude of the Kerr constant and the incident light intensity. Here, we consider the case when both the Kerr effect and the GVD are significant. Requiring that Eqs. (4.22) and (4.24) are consistent with each other determines the phase parameter d:

$$d = \frac{3a}{2}\left(\frac{\mu^2 \Omega''}{\hbar^2 V^2 n_L} - 1\right) \Bigg/ \left(\frac{2\tau\mu^2}{n_L \hbar^2} + \delta_a\right). \tag{4.25}$$

Similarly, in order for Eqs. (4.21) and (4.23) to be consistent with each other the wave vector shift k must obey the equation

$$\xi^3 + \xi^2\left(\frac{2\tilde{\delta}_a}{V} - V\right) + \xi\left[2\tilde{\delta} - 4\tilde{\delta}_a + \left(\frac{\tilde{\delta}_a}{V}\right)^2\right] - 2V\tilde{\delta} + 2V\tilde{\delta}_a - \frac{\tilde{\delta}_a^2}{V} - \frac{\eta\mu^2}{V\hbar\beta^2} = 0, \tag{4.26}$$

where $\xi = k/\beta$, $\tilde{\delta} = \delta/\beta$, and $\tilde{\delta}_a = \delta_a/\beta$. Equation (4.26) determines the wave vector shift k for a given detuning δ and velocity V. The soliton velocity and detuning are free parameters with the restriction that they are small compared to unity in the near band-edge approximation. We make the observation from Eq. (4.26) that when $V \to -V$, $\xi \to -\xi$. Since $\tau = \Omega'' k/V - 1 > 0$, k and V must have the same sign. Equation (4.26) always has one real root and in certain cases three real roots. Our numerical study reveals that when there are three real roots only one of them leads to a physically admissible soliton solution.

The solution described here is quite different from the fiber SIT-NLS solution obtained for pulse propagation in a doped optical fiber [14]. In fibers, GVD arises from the material dispersion, whereas in the Bragg grating a much larger GVD arises from the variation in the linear dielectric constant. A more important difference is that in fibers, in the absence of phase modulation, the existence of the SIT-NLS solution requires that the material constants satisfy the relation $\Omega'' = n_L \hbar^2/\mu^2$ [14]. In the SIT-gap solution this highly restrictive condition on the material parameters is not required. In this sense, our SIT-gap soliton is much more robust than previously studied [14] SIT fiber solitons.

In the case of erbium doped fibers, the typical value of $n_L \hbar^2/\mu^2$ turns out to be many orders higher than the value of Ω'' in the fibers. This makes the realization of such a soliton in erbium doped fibers very difficult. Our studies suggest that a fiber engineered with a periodic grating would greatly facilitate the observation of a SIT-NLS soliton soliton with erbium atoms.

Before discussing the SIT-gap soliton solution in more detail we briefly review the important properties of the gap solitary wave when there are no dopant atoms in the medium. When the dopant density parameter $\eta = 0$, the soliton inverse size parameter is given by

$$a^2 = \frac{2V^2}{\Omega''}\alpha = \frac{2V^2}{\Omega''}(\delta + k^2\Omega''/2) \tag{4.27}$$

and the soliton amplitude becomes

$$A^2 = \frac{a^2 \Omega''}{3 n_L V^2}. \tag{4.28}$$

Here, $\tau = (\Omega'' k/V - 1) = 0$. This determines the wave vector shift for a given soliton velocity V. The gap solitary wave is described by two free parameters, the soliton velocity V and the detuning δ. From Eq. (4.27) it can be seen that a vanishes as $\delta \to -k^2\Omega''/2$. In other words, the soliton size diverges and the amplitude vanishes just outside the PBG. When $V = 0$, the soliton is stationary and the soliton amplitude vanishes precisely when the detuning δ approaches the upper band edge. The near band-edge solution agrees with the more general time-dependent solution obtained by Aceves and Wabnitz [6] for an undoped material, in the limit when $V, \delta \ll 1$.

In order to illustrate the SIT-gap solution further, we consider the following material parameters: $\mu = 10^{-19}$ (esu), $\beta \equiv \Delta\epsilon/4\tilde{\epsilon} = 0.1$, and $n_L = 6\pi\chi^{(3)}/\tilde{\epsilon} = 10^{-9}$ (esu). A particularly simple solution is obtained when the pulse velocity is chosen to satisfy the relation $V = \mu\sqrt{(\Omega''/n_L)}/\hbar$. For this velocity it is readily seen from Eq. (4.25) that the phase modulation $\phi = 0$. Below we will describe in detail this particular case ($V = 0.0079$) and then make some generalizations to $\phi \neq 0$. Consider first the case in which the atomic transition frequency is at the upper band edge $\omega_{ba} = 1 + \beta$ and a dopant density $\eta = 10^{16}$ cm^{-3}. In this case, the atomic detuning simply becomes $\tilde{\delta}_a = \Omega'' \delta_a = -\tilde{\delta}$. The soliton disappears just outside the PBG at $\tilde{\delta} \simeq -0.000\,129$ with $\tilde{k} \simeq 0.011\,65$. However, the soliton solution exists further outside the band gap region than the pure undoped gap soliton, with the same velocity. When $\tilde{\delta} \simeq -0.000\,129$, there are three real roots $\tilde{k}$ given by 0.0038, -0.014, and 0.0187. The first two make $a^2 < 0$, so that only the third is physically admissible. For $\tilde{\delta} = 0$, there is only one real root 0.0134 making $a^2 > 0$. In Fig.

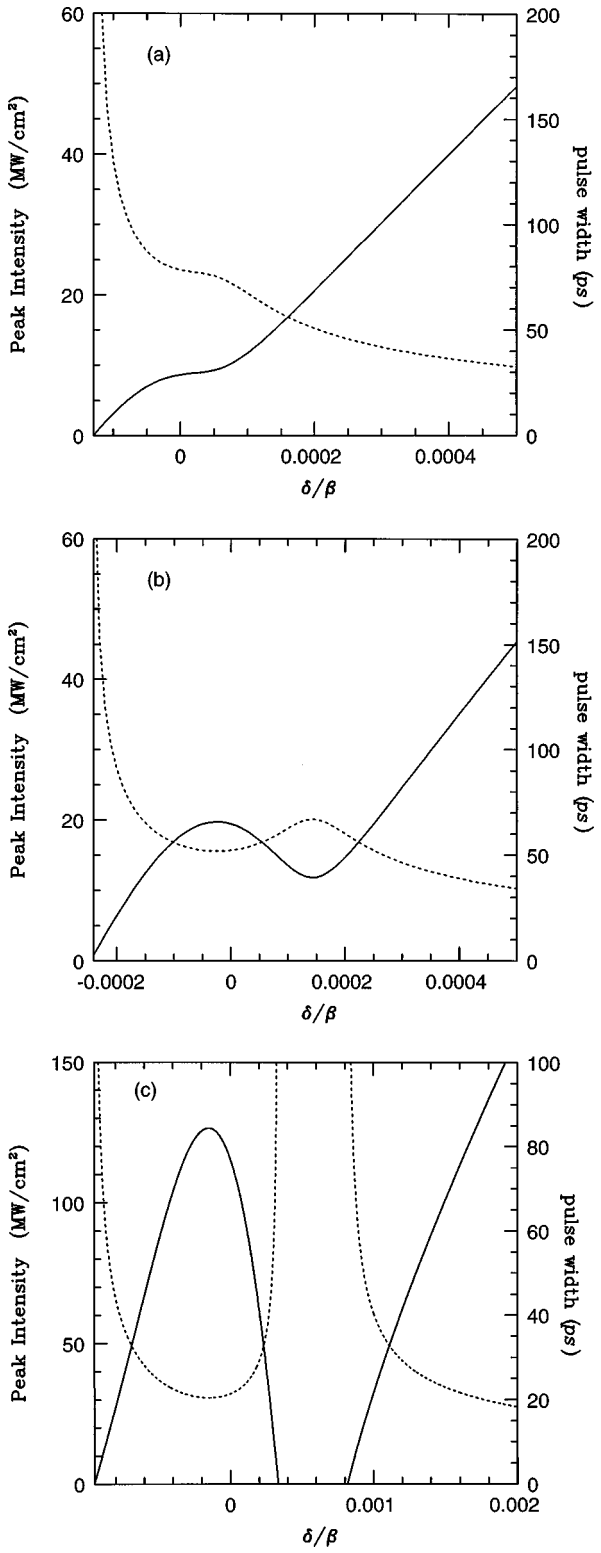

FIG. 7. Shown is the peak intensity (solid line) and pulse width (dotted line) as a function of the detuning from the upper band edge for (a) $\eta=10^{16}\ \mathrm{cm}^{-3}$, (b) $\eta=5\times10^{16}\ \mathrm{cm}^{-3}$, and (c) $\eta=10^{18}\ \mathrm{cm}^{-3}$. The detuning parameter $\delta/\beta>0$ corresponds to a detuning inside the band gap whereas $\delta/\beta<0$ corresponds to a detuning outside the photonic band gap. Here the atomic transition frequency $\omega_{ba}=1+\beta$ is assumed to be at the upper band edge and the other material parameters are chosen as $\beta=0.1$, $\tilde{\epsilon}=3$, $\mu=10^{-19}$ (esu), $V=0.0079$, and $n_L=10^{-9}$ (esu).

7(a) the peak intensity and width of the SIT-gap soliton solution is plotted as a function of the detuning $\tilde{\delta}$. As can be seen the peak intensity increases and the width becomes shorter as the soliton frequency is detuned into the band gap region just below the upper band edge ($\tilde{\delta}>0$). Qualitatively similar results hold when the atomic transition frequency is placed just below the upper band edge ($\omega_{ba}=1+0.999\beta$) with the same density of atoms. Here the soliton vanishes at around $\tilde{\delta}\simeq-3.0\times10^{-5}$ with $\tilde{k}\simeq0.007\,965$, similar to the pure gap soliton case. The results are depicted in Fig. 8(a).

Dramatic changes are observed in the solution when the atomic transition frequency is placed slightly above the upper band edge ($\omega_{ba}=1+1.0001\beta$). In this case, the soliton vanishes at $\tilde{\delta}\simeq-0.000\,194$ with $\tilde{k}\simeq0.014\,89$. As shown in Fig. 9(a) the soliton width first narrows, then widens, and finally continues to narrow again. This behavior has no analog in the pure gap soliton solution. As the atomic transition frequency is tuned further above the upper band edge ($\omega_{ba}=1+1.1\beta$), the minimum point in the intensity of Fig. 9(a) eventually goes to zero, splitting the solution into two frequency bands, $-0.100\,012<\tilde{\delta}<-0.099\,988\,1$ and $-0.311\times10^{-4}<\tilde{\delta}$. In other words, the parameter space in which a soliton solution exists is divided into two regions. This fact is easily seen by setting a equal to zero in Eqs. (4.21) and (4.23). From Eq. (4.21) we find that

$$\tilde{\delta}=-\frac{\tilde{\delta}_d(\tilde{k}/V-1)+\tilde{k}^2/2}{(2-\tilde{k}/V)}. \tag{4.29}$$

Here, we have assumed that the transition frequency is $\omega_{ba}=1+\beta-\delta_d$. Inserting $\tilde{\delta}$ into Eq. (4.23) leads to the following nonlinear equation for $\tilde{k}$:

$$(\tilde{k}/V-1)(\tilde{\delta}_d+\tilde{k}^2/2)^2-\frac{\eta\mu^2}{\hbar\beta^2}(2-\tilde{k}/V)^2=0. \tag{4.30}$$

Depending on the choice of material parameters and soliton velocity, Eq. (4.30) may have one or more real roots, leading to a region where a soliton solution exists. Clearly, when there are no dopant atoms ($\eta=0$), then the only possible root is $\tilde{k}=V$.

Next we consider how changes in the density of the dopant atoms lead to changes in the soliton structure. We begin with the case when the atomic transition frequency is precisely at the band edge. As the dopant density is increased to $\eta=5\times10^{16}\ \mathrm{cm}^{-3}$ the small flat region in the peak intensity in Fig. 7(a) of the solution becomes more pronounced and evolves into the dip seen in Fig. 7(b). As the dopant density is further increased the peak intensity vanishes over a small frequency range, causing the solution to split. We show this effect in Fig. 7(c) for a dopant density $\eta=10^{18}\ \mathrm{cm}^{-3}$. As can be seen, there is a soliton solution between $0.000\,334<\tilde{\delta}<0.000\,817$, and the solution vanishes at either end point of this frequency interval. In addition the soliton disappears for $\tilde{\delta}\leqslant-0.000\,946\,3$. For the case when the atomic transition frequency is placed just below the upper band edge, for $\eta=10^{16}\ \mathrm{cm}^{-3}$ we see from Fig. 8(a) there are no dips in the

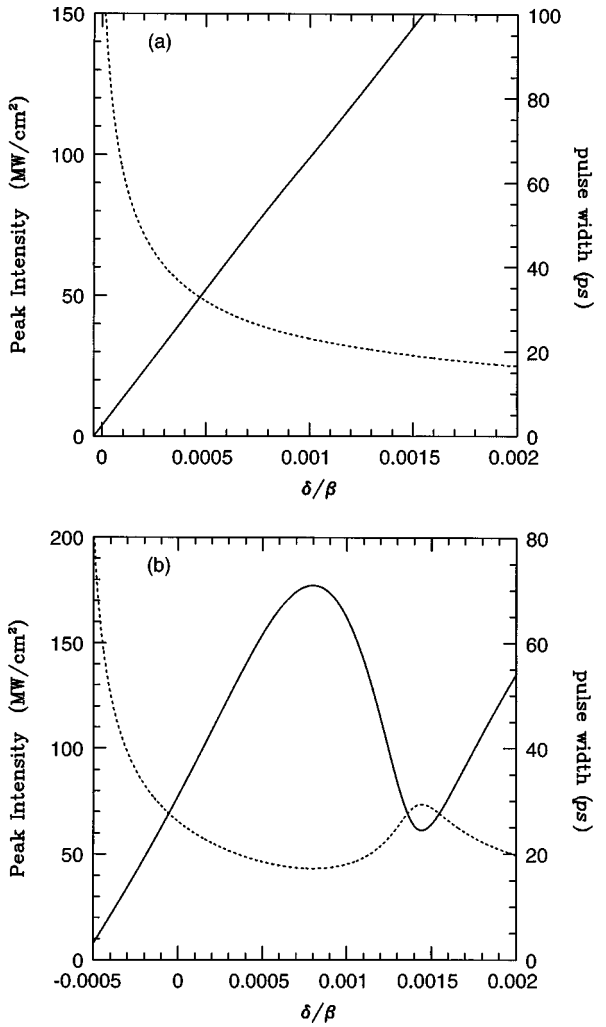

FIG. 8. Plotted is the peak intensity (solid line) and pulse width (dotted line) as a function of the detuning δ/β from the upper band edge, when the atomic transition frequency is chosen to be slightly below the upper band edge and inside the gap $\omega_{ba}=1+0.999\beta$. (a) For a density $\eta=10^{16}$ cm^{-3} and (b) for $\eta=10^{18}$ cm^{-3}. All other parameters are the same as in Fig. 7.

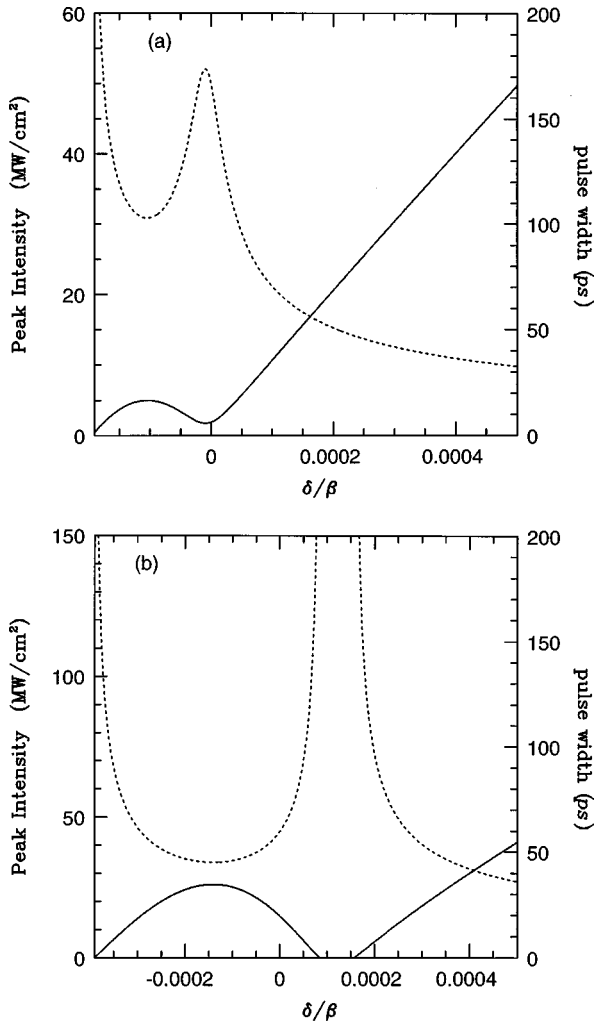

FIG. 9. Plotted is the peak intensity (solid line) and pulse width (dotted line) of soliton solution when the atomic transition frequency is slightly outside the band gap $\omega_{ba}=1+1.0001\beta$. (a) For a density $\eta=10^{16}$ cm^{-3} and (b) for $\eta=10^{17}$ cm^{-3}. All other parameters are the same as in Fig. 7.

solution. However, when the density is increased to $\eta=10^{18}$ cm^{-3}, there is a significant change in the solution [see Fig. 8(b)]. Similar effects occur when the transition frequency is slightly outside the band gap [see Fig. 9(b)]. Clearly the atomic transition frequency as well as the dopant density together have a significant effect on the nature of the SIT-gap solution. For the pure gap soliton there are only two free parameters (V,δ) describing the solution. For the SIT-gap solution the atomic detuning frequency and dopant density are degrees of freedom leading to a much richer family of soliton solutions.

So far we have fixed the atomic transition frequency, and then varied the soliton average frequency by changing the laser frequency. Another situation with interesting practical applications arises when the average soliton frequency is fixed and the atomic detuning frequency δ_a is varied. This can be accomplished by applying a static electric field across the medium and Stark shifting the atomic transition frequency. Consider first the case when $\tilde{\delta}=0$ and $\eta=10^{16}$ cm^{-3}. Here we define the atomic transition frequency as $\omega_{ba}=1+\beta-\delta+\Delta$, where δ is fixed at some value and Δ represents the atomic detuning ($\Delta>0$ shifts the frequency outside the band gap region and $\Delta<0$, inside the band gap). The peak intensity and pulse width as a function of the detuning Δ are shown in Fig. 10(a). Clearly, the soliton parameters change very dramatically around $\Delta\simeq 0$ for a small shift in Δ. This suggests that the soliton characteristics can be controlled externally by an applied static electric field. Soliton gating and control in this manner may be very useful in optical telecommunications and optical computing. In Fig. 11(a) the results are shown when the average soliton frequency is placed inside the band gap ($\tilde{\delta}=0.001$). The variation in soliton peak intensity and pulse width requires a larger change in Δ values and the variation is weaker compared with the band-edge case ($\tilde{\delta}=0$). In addition the change in the solution now appears more on the negative side of Δ. As before, the atomic density has an important effect on the results.

When $\tilde{\delta}=0$, as the dopant density is increased, the mini-

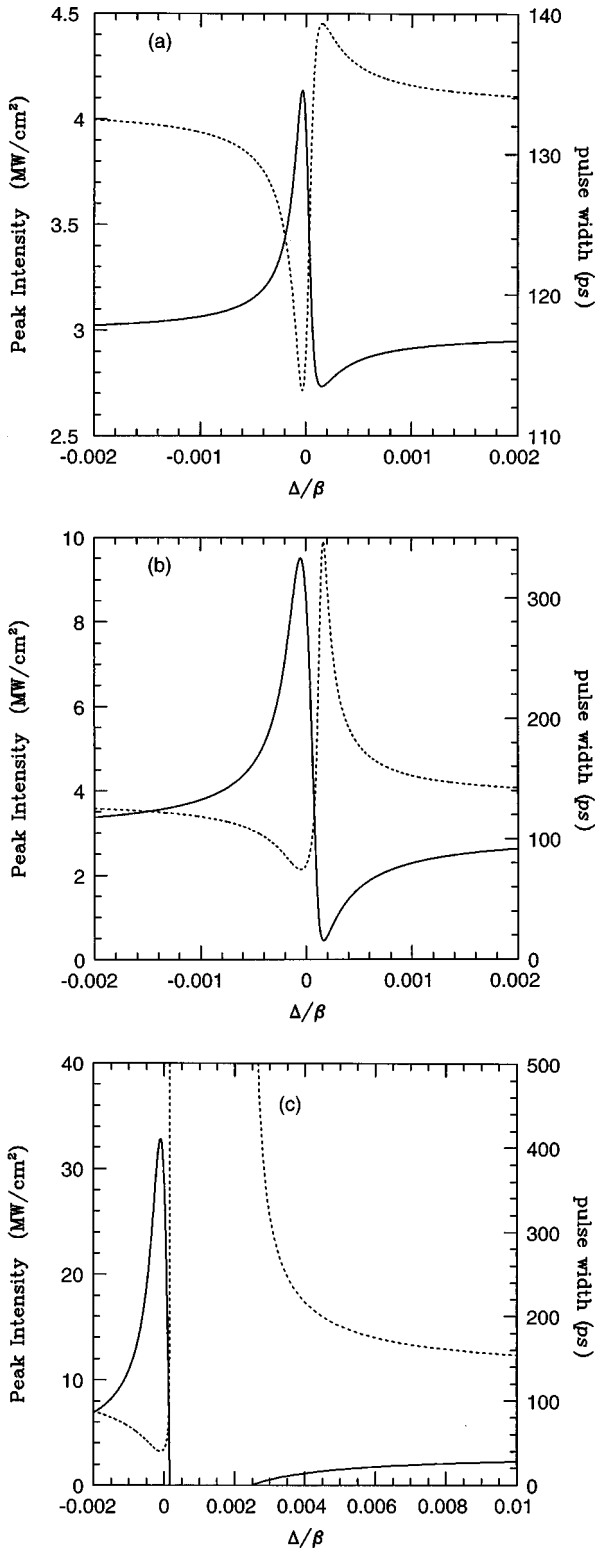

FIG. 10. Plotted is the peak intensity (solid line) and pulse width (dotted line) as a function of the atomic detuning Δ/β from the on resonance case. Here the detuning $\delta/\beta=0$. (a) for $\eta=10^{15}$ cm^{-3}, (b) for $\eta=10^{16}$ cm^{-3}, (c) $\eta=10^{17}$ cm^{-3}. All other parameters are the same as in Fig. 7.

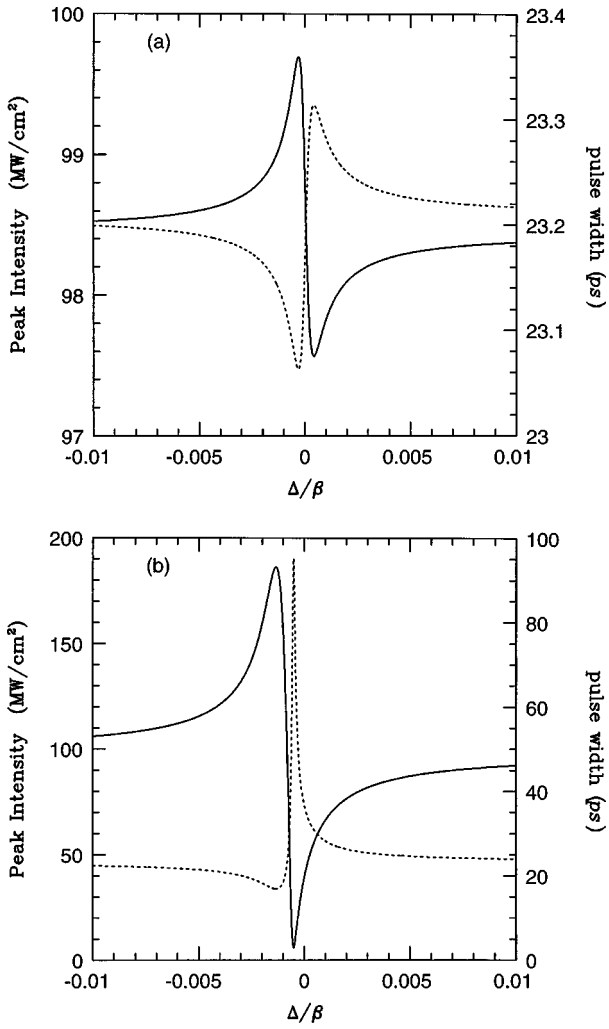

FIG. 11. Plotted is the peak intensity (solid line) and pulse width (dotted line) as a function of Δ/β for $\delta/\beta=0.001$. (a) $\eta=10^{16}$ cm^{-3} and (b) $\eta=9.0\times10^{17}$ cm^{-3}. All other parameters are the same as in Fig. 7.

mum point in the intensity approaches the axis and at some density crosses it. In Fig. 10(c) we show the results for $\eta=10^{17}$ cm^{-3}. There is no soliton solution in the range $0.000\,127\,7<\tilde{\delta}<0.002\,461$, at velocity $V=0.0079$. On the other hand, soliton solutions with phase modulation and different velocity do exist in this quasi-stop-band for the same atomic density. This fixed velocity stop-band effect disappears when the dopant density is lowered to $\eta=10^{15}$ cm^{-3} [Fig. 10(a)]. When $\tilde{\delta}=0.001$ and $\eta=9.0\times10^{17}$ cm^{-3} we show in Fig. 11(b) that the increase of the dopant density has a stronger effect on the soliton parameters than in Fig. 11(a). In particular, the minimum point of the intensity is closer to zero. Further increase of the dopant density eventually splits the solution into two regions as shown in Fig. 10(c). In all cases the choice of dopant density and the value of the average soliton frequency have a significant effect on the soliton parameters, as the atomic transition frequency is varied. These results underscore the high degree of tunability of soliton properties, in the doped PBG, by means of an external electric field.

In the illustrations given above, it was assumed that the velocity is chosen such that the phase modulation $\phi=0$. This assumption facilitated a simple analytical treatment of soliton properties. As phase modulation is introduced the soliton velocity deviates from the special value of V

$=\mu\sqrt{\Omega''}/\hbar\sqrt{n_L}$ and a new family of soliton solutions emerges for each choice of V. We may consider $\phi=0$ as a special case from which more general solutions are obtained perturbatively with small $\partial\phi/\partial t$ and small deviations in velocity. This special case facilitates the analytical treatment of inhomogeneous line broadening and the pulse area theorem as we discuss below. The description of more general solitons exhibiting phase modulation, however, requires the use of numerical methods.

The population inversion w and the induced polarization components u and v for the $\phi=0$ case are

$$\overline{w}=-1+\frac{2}{1+(\delta_a/a)^2}\,\mathrm{sech}^2(a\zeta), \tag{4.31}$$

$$v=-\frac{1}{\sqrt{3}}\frac{\mu}{1+(\delta_a/a)^2}\,\mathrm{sech}(a\zeta)\tanh(a\zeta), \tag{4.32}$$

$$u=-\frac{1}{\sqrt{3}}\frac{\mu\delta_a/a}{1+(\delta_a/a)^2}\,\mathrm{sech}(a\zeta). \tag{4.33}$$

Since v can be written as $v(\zeta,\delta_a)=f(\delta_a)v(\zeta,0)$ we may use the factorization method to obtain the solution when inhomogeneous line broadening is taken into consideration. In particular,

$$f(\delta_a)=\frac{1}{1+(\delta_a/a)^2}. \tag{4.34}$$

We define

$$I_1=\int_{-\infty}^{\infty}g(\delta_a'-\delta_a)f(\delta_a)d(\delta_a) \tag{4.35}$$

and

$$I_2=\int_{-\infty}^{\infty}\delta_a g(\delta_a'-\delta_a)f(\delta_a)d(\delta_a), \tag{4.36}$$

where $g(\delta_a'-\delta_a)$ is the probability distribution of the inhomogeneously broadened energy levels. Then Eq. (4.21) must be replaced by

$$\frac{a^2\Omega''}{2V^2}=\alpha+\frac{I_2}{I_1}\tau \tag{4.37}$$

and Eq. (4.23) replaced by

$$a^2\tau=\frac{\eta\mu^2}{\hbar}I_1. \tag{4.38}$$

Here, $\tau=\Omega''k/V-1$. In the sharp-line limit [when $g=\delta(\delta_a'-\delta_a)$ is a delta function] we recover the previous solution.

SIT solitons in ordinary vacuum satisfy the well known McCall-Hahn pulse area theorem [9]. A similar area theorem holds for the doped Bragg grating. This can be seen by considering the on resonance case. Then $u=0$ and the Bloch equations take the form $\dot{v}=-(\mu^2/\hbar)\varepsilon\overline{w}$ and $\dot{\overline{w}}=(12/\hbar)\varepsilon v$.

These equations can be mapped onto the standard type of Bloch equations by defining $R=2\sqrt{3}\mu\varepsilon/\hbar$ and $\overline{v}=2\sqrt{3}v/\mu$, then we have $\dot{\overline{v}}=-R\overline{w}$ and $\dot{\overline{w}}=R\overline{v}$.

The Bloch vector tipping angle is defined as $\Theta(x,t)=\int_{-\infty}^{t}dt'R(x,t')=(2\sqrt{3}\mu/\hbar)\int_{-\infty}^{t}dt'\varepsilon(x,t')\equiv$(pulse area). Then we have the solution $\overline{v}=-\sin(\Theta)$ and $\overline{w}=-\cos(\Theta)$. In the $(\overline{u},\overline{w})$ plane the atoms are initially in their ground state $\overline{w}(-\infty)=-1$ and are subsequently excited as the pulse propagates through the medium. Finally they return back to their ground state. The Bloch vector tipping angle rotates through 2π, so that the area of these pulses is 2π as well.

The McCall-Hahn pulse area theorem describes how an arbitrary optical pulse evolves into a pulse area given by an integer multiple of 2π. Introducing the rescaling $x/\Omega''k\rightarrow x$ in Eq. (4.7) we obtain

$$\frac{\partial\varepsilon(x,t)}{\partial t}+\frac{\partial\varepsilon(x,t)}{\partial x}+\eta\langle v(x,t,\delta_a)\rangle=0, \tag{4.39}$$

where the $\langle\ \rangle$ bracket in Eq. (4.39) represents the spectral averaging over the inhomogeneously broadened atomic line. The Bloch equations can be expressed as

$$\frac{\partial u}{\partial t}=-\delta_a v, \tag{4.40}$$

$$\frac{\partial v}{\partial t}=\delta_a u-\frac{\mu^2}{\hbar}\varepsilon\overline{w}. \tag{4.41}$$

Integrating Eq. (4.39) over the the time of the pulse and multiplying by $2\sqrt{3}\mu/\hbar$, we obtain

$$\frac{\partial A(x)}{\partial x}=-\frac{2\sqrt{3}\mu\eta}{\hbar}\int_{-\infty}^{T}\langle v(x,t,\delta_a)\rangle dt, \tag{4.42}$$

where the pulse area is defined as $A(x)=\Theta(x,T)$. The upper limit T is large enough for the envelope $\varepsilon(x,t)$ to be effectively zero. For a time interval $T>t>T_0$ the second term in Eq. (4.41) is negligible, where T_0 marks the end of the pulse. Then we obtain a solution $u(T_0,x,\delta_a)=-v\,\sin(\delta_a t)$. Also from Eq. (4.40) $v=-(1/\delta_a)(\partial u/\partial t)$. Using these solutions in Eq. (4.42) we obtain

$$\frac{\partial A(x)}{\partial x}=\frac{2\sqrt{3}\mu\eta}{\hbar}\int_{-\infty}^{\infty}g(\delta_a)v(x,t,\delta_a)\frac{\sin(\delta_a t)}{\delta_a}d(\delta_a). \tag{4.43}$$

Since the incoherent relaxation times are assumed to be infinite in this model we can take the limit that $T\rightarrow\infty$. Then $\sin(\delta_a t)/\delta_a$ acts as a delta function and the area theorem becomes

$$\frac{\partial A(x)}{\partial x}=\frac{2\sqrt{3}\mu\eta\pi}{\hbar}g(0)v(0,x,T_0)=-\frac{\mu\eta\pi}{\hbar}g(0)\sin A(x). \tag{4.44}$$

The general solution is given by

$$A(x)=2\arctan\left[\tan[A(0)/2]\exp\left(-\frac{\mu\eta\pi}{2\hbar}x\right)\right]. \quad (4.45)$$

As in the case of ordinary vacuum, this area theorem shows that optical pulses with arbitrary pulse areas will evolve into pulses with areas that are multiples of 2π for which $\partial A(x)/\partial x=0$.

B. Solitary waves in a linear Bragg grating doped with resonance two-level atoms

In some cases, it is possible that the doped PBG material exhibits negligible nonresonant Kerr response. For example, in semiconductor materials such as AlGaAs, the Kerr coefficient changes sign between 0.8 and 1.6 μm. By operating close to the zero value, Kerr interaction may then be neglected. When $n_L=0$ Eqs. (4.21)–(4.24) take the form

$$a^2=\frac{2V^2}{\Omega''}(\alpha+\tau\delta_a), \quad (4.46)$$

$$d=\frac{3\Omega''a}{4V^2\tau}, \quad (4.47)$$

$$\tau(a^2+\delta_a^2)=\frac{\eta\mu^2}{\hbar}, \quad (4.48)$$

$$A^2=\frac{\hbar^2}{3\mu^2}\left(a^2+\frac{2}{3}\delta_a da\right). \quad (4.49)$$

Here, the phase parameter d is directly determined by Eq. (4.47) and is nonzero for any velocity and detuning. From Eqs. (4.46) and (4.48) we obtain the same cubic equation (4.26) as in the SIT-gap solution for a given soliton velocity V. The above solution is valid when the phase parameter d is much less than unity. This is achieved when the frequency detuning δ is close to the critical detuning where the solution vanishes.

We illustrate the solution using the following material parameters: $\mu=10^{-19}$ (esu), $\eta=10^{16}$ cm^{-3}, and $\beta=0.1$. Consider a soliton velocity of $V=0.02$. In this case the soliton vanishes around $\tilde{\delta}=-0.000\,273\,44$ for $\tilde{k}=0.0221$.

The atomic Bloch vector components $\bar{w}$, v, and u are given by

$$\bar{w}=-1+\frac{6\tau A^2}{\hbar\eta}\,\mathrm{sech}^2(a\zeta), \quad (4.50)$$

$$v=-\frac{\tau A a}{\eta}\tanh(a\zeta)\mathrm{sech}(a\zeta), \quad (4.51)$$

$$u=-\frac{a\tau\delta_a}{\eta}A\,\mathrm{sech}(a\zeta)-\frac{A}{\eta}\left(\tau a d-\frac{\Omega''a^2}{V^2}\right)\mathrm{sech}^3(a\zeta). \quad (4.52)$$

Clearly the atomic Bloch vector has a structure similar to that of SIT in a uniform Kerr medium. In u, the contribution proportional to sech^3 is entirely due to the GVD effect. In this sense the role of the Kerr effect is replaced here by the GVD.

C. Solitary wave solution in the presence of damping and linear loss/gain

In obtaining a solitary wave solution in the preceding section, it was assumed that the pulse duration $\tau\ll T_1, T_2$, so that no damping occurs for the duration of the pulse. In this case we set $T_{1,2}\to\infty$. As discussed before, for atoms doped in a solid material the lifetime of the upper state is on the order of ms to μs. For pulses with nanosecond to picosecond durations, we may neglect $1/T_1$. On the other hand, the dipole-dephasing time T_2 can be on the order of nanoseconds to picoseconds. One possible way to prolong T_2 is to cool the material to liquid He^4 temperatures. If the pulse duration is comparable to the dephasing time T_2, the Bloch equation does not allow a shape preserving pulse. Some other mechanism is needed to compensate this decoherence. In this section we demonstrate the existence of solitary wave solutions, in the presence of linear loss/gain of the host medium and incoherent pumping of the medium. We consider a model with nonresonant Kerr nonlinearity in which the field is tuned close to the band edge. For illustration, we consider the on resonance case ($\delta_a=0$) and $\phi=0$. Then $u=0$ and setting the phase $\phi=0$, in Eqs. (4.13)–(4.17) we obtain

$$\frac{\Omega''}{2V^2}\ddot{\varepsilon}-\alpha\varepsilon+3n_L\varepsilon^3=0, \quad (4.53)$$

$$-\tau\dot{\varepsilon}+\Gamma\varepsilon+\eta v=0, \quad (4.54)$$

$$\dot{v}=-\frac{\mu^2}{\hbar}\varepsilon\bar{w}-\frac{v}{T_2}, \quad (4.55)$$

$$\dot{\bar{w}}=\frac{12}{\hbar}\varepsilon v. \quad (4.56)$$

Equation (4.53) is just the nonlinear Schrödinger equation which has the solution $\varepsilon=A\,\mathrm{sech}(a\zeta)$ with pulse width

$$a=\sqrt{\frac{2\alpha}{\Omega''}}\,V \quad (4.57)$$

and amplitude

$$A=\sqrt{\frac{\Omega''}{3n_L}}\frac{a}{V}. \quad (4.58)$$

Inserting v from Eq. (4.54) in Eq. (4.56) we obtain

$$\int_{-\infty}^{\zeta}\dot{\bar{w}}(\zeta')d\zeta'=\int_{-\infty}^{\zeta}\frac{12}{\hbar\eta}(\tau\varepsilon\dot{\varepsilon}-\Gamma\varepsilon^2)d\zeta'. \quad (4.59)$$

The left hand side can easily be integrated using the initial condition $w(-\infty)=w_{\mathrm{in}}$ and the right hand side can be integrated using the envelope function ε found above:

$$\bar{w}(\zeta)=w_{\mathrm{in}}-\frac{12\Gamma A^2}{\eta\hbar a}+\frac{6\tau A^2}{\eta\hbar}\,\mathrm{sech}^2(a\zeta)-\frac{12\Gamma A^2}{\eta\hbar a}\tanh(a\zeta). \quad (4.60)$$

Equation (4.54) yields the atomic polarization

$$v=-\frac{\tau aA}{\eta}\,\mathrm{sech}(a\zeta)\tanh(a\zeta)-\Gamma A\,\mathrm{sech}(a\zeta). \quad (4.61)$$

Inserting Eqs. (4.60) and (4.61) into Eq. (4.55) and then equating terms proportional to sech, sech tanh and sech^3, we obtain the following set of conditions:

$$\frac{\tau a^2}{\eta}=-\frac{\mu^2 w_{\mathrm{in}}}{\hbar}+\frac{\mu^2 12\Gamma A^2}{\eta\hbar^2 a}+\frac{\Gamma}{T_2\eta}, \quad (4.62)$$

$$\tau a^2=\frac{3\mu^2\tau A^2}{\hbar^2}, \quad (4.63)$$

$$\Gamma a=\frac{12\Gamma\mu^2A^2}{\hbar^2 a}+\frac{\tau a}{T_2}. \quad (4.64)$$

Combining Eqs. (4.63) and (4.64) we obtain the relation

$$\tau\left(3\Gamma+\frac{\tau}{T_2}\right)=0. \quad (4.65)$$

From Eq. (4.65) there are two possible solutions, $\tau=0$ and $\tau=-3\Gamma T_2$. These two values for τ yield two distinct solitary wave solutions.

When $\tau=0$, Eq. (4.64) yields the amplitude

$$A=\frac{a\hbar}{2\sqrt{3}\mu} \quad (4.66)$$

and Eq. (4.62) yields the inverse pulse width

$$a=\frac{\eta\mu^2 w_{\mathrm{in}}}{\hbar\Gamma}-\frac{1}{T_2}. \quad (4.67)$$

We can see from Eq. (4.66) that the pulse area is $(2\sqrt{3}\mu/\hbar)\int\varepsilon(\zeta)d\zeta=\pi$. The amplitudes obtained from Eq. (4.58) and Eq. (4.66) are consistent provided that the velocity

$$V=\frac{2\mu}{\hbar}\sqrt{\frac{\Omega''}{n_L}}. \quad (4.68)$$

Since $\tau=(\Omega''k/V-1)=0$, it follows that $k=V/\Omega''$. Using V from Eq. (4.68) we obtain

$$k=\frac{V}{\Omega''}=\frac{2\mu}{\hbar}\sqrt{\frac{1}{\Omega'' n_L}}. \quad (4.69)$$

Equation (4.57) gives the pulse width which can be expressed, using Eqs. (4.68) and (4.69), as

$$a=\frac{4\mu^2}{\hbar^2 n_L}. \quad (4.70)$$

Since a was already determined from Eq. (4.67) consistency requires that the initial inversion is given by

$$w_{\mathrm{in}}=\frac{4\Gamma}{\eta\hbar n_L}+\frac{\hbar\Gamma}{\eta\mu^2 T_2}. \quad (4.71)$$

In other words, the incoherent pumping has to be chosen to satisfy the condition (4.71). Let us consider a numerical example. Γ is related to the linear absorption coefficient by the relation $\Gamma=\epsilon_i/4\tilde{\epsilon}$, where ϵ_i is the imaginary part of the dielectric constant and $\tilde{\epsilon}$ is the real part of the dielectric constant. In the literature the linear absorption is defined through the linear absorption coefficient $\alpha=(\omega/c)\mathrm{Im}\,\chi$ in units of cm^{-1}. With this definition $\Gamma=10^{-5}\alpha/4\tilde{\epsilon}$, where we assumed that $\omega=10^{15}$ s^{-1}. Consider an erbium doped fiber grating. The material parameters are approximately given as $\mu=10^{-21}$ (esu), $n_L=10^{-14}$ (esu), $T_2=0.1$ ps, $\eta=10^{18}$ cm^{-3}, and $\alpha=10^{-6}$ cm^{-1}. Then we require that $w_{\mathrm{in}}=0.01$.

In the limit when $T_2\to\infty$ in a medium with linear loss ($\Gamma>0$), the condition (4.71) reduces to

$$w_{\mathrm{in}}=\frac{4\Gamma}{\eta\hbar n_L}. \quad (4.72)$$

Such an initial population can be prepared by incoherent pumping of the atoms provided that the material parameters satisfy the inequality $\Gamma<\hbar\eta n_L/4$. In this case, the population inversion can be written as

$$\overline{w}(\zeta)=-w_{\mathrm{in}}\tanh(a\zeta). \quad (4.73)$$

An alternative solution is possible when $\tau=-3\Gamma T_2$. In this case, $k=(V/\Omega'')(1-3\Gamma T_2)$. From Eq. (4.63) the amplitude is given by

$$A^2=\frac{\hbar^2 a^2}{3\mu^2}. \quad (4.74)$$

For this solution, the pulse area is equal to 2π rather than π. Demanding the consistency of Eqs. (4.74) and (4.58) yields a velocity

$$V=\frac{\mu}{\hbar}\sqrt{\frac{\Omega''}{n_L}}, \quad (4.75)$$

which is precisely one-half of the velocity of the $\tau=0$ soliton. The soliton wave vector is given by

$$k=\sqrt{\frac{\mu^2}{\Omega''\hbar^2 n_L}}\,(1-3\Gamma T_2) \quad (4.76)$$

and the inverse pulse width follows from Eq. (4.57):

$$a=\frac{2\mu^2}{\hbar^2 n_L}\left(\frac{\mu^2}{2\hbar^2 n_L}(1-3\Gamma T_2)^2\right). \quad (4.77)$$

On the other hand, Eq. (4.62) yields

$$a=-\frac{2}{3T_2}+\sqrt{\left(\frac{2}{3T_2}\right)^2+\frac{1}{3T_2}\left(\frac{\eta\mu^2 w_{\mathrm{in}}}{\Gamma}-\frac{1}{T_2}\right)}. \quad (4.78)$$

In this case, the consistency of Eqs. (4.77) and (4.78) leads to a more complicated relation between the material parameters and the incoherent pumping:

$$w_{\rm in}=\frac{3T_2\Gamma}{\eta\mu^2}\left[\frac{2\mu^2}{\hbar^2 n_L}\left(\frac{\mu^2}{2\hbar^2 n_L}(1-3\Gamma T_2)^2+\frac{2}{3T_2}\right)^2 -\left(\frac{2}{3T_2}\right)^2+\frac{1}{3T_2^2}\right]. \tag{4.79}$$

V. DISCUSSION AND CONCLUSIONS

We have shown the existence of self-induced transparency solitary waves in a one-dimensional PBG doped with resonant two-level atoms. A rich variety of soliton solutions are possible depending where the incident light frequency is tuned relative to the photonic band edges and the nonlinear response of the host medium. Specifically we demonstrated that near the band edge, there exist a family of solutions that is simultaneously a gap soliton as well as a self-induced transparency soliton. These solutions depend strongly on the atomic transition frequency as well as the dopant concentration. Analytical solutions are possible for a particular soliton velocity for which self-phase modulation effects vanish. In general, it is necessary to use numerical methods to obtain solutions valid for general velocities and general phase modulation effects. The near band-edge approximation provides a valuable starting point for the description of solitons deeper inside the photonic band gaps.

We have restricted our attention to a number of special and illustrative cases where simple analytical solutions are possible. We believe that these illustrations provide an introduction to the rich variety of soliton solutions which arise in a doped photonic band gap material. The most striking feature of the near band-edge solitons is their very high degree of tunability through small changes in the atomic transition frequencies and atomic densities. In providing these illustrations, we have made a number of idealizations in our model which we discuss below.

A more realistic model of SIT-gap solitons must include the effects of inhomogeneous line broadening of the dopant atoms. For dopant atoms embedded in the solid fraction of the material, random Stark shifts of the excited energy levels will arise from the local electric fields of the crystal. For real impurity atoms such as erbium, there are many atomic transitions close to each other in frequency. It is important to generalize our two-level model to dopant atoms with several closely spaced excited levels for comparison with experiments. Another useful generalization is to the case of electronic excitations in a semiconductor host material. In semiconductors, the bound excitations can be modeled as two-level systems which move with the optical pulse.

In this paper we have considered only a one-dimensional periodic structure. In a real three-dimensional PBG material, transverse propagation effects must be included to describe finite energy soliton pulses of finite extent in all spatial dimensions. From an experimental point of view it is important to understand the stability of SIT-gap solitons with respect to small perturbations. It is also useful to study pulse propagation in a finite resonant medium, how to excite these solitons in a finite medium, and whether an arbitrary pulse evolves into a stable SIT-gap soliton.

It is our hope that our simple model calculations will motivate more detailed numerical studies of this nature which explore the full parameter space of soliton solutions in a PBG. This may in turn lead to the application of doped PBG materials for all-optical switching devices and fiber interconnectors for pulse reshaping and amplification in all-optical communication systems.

ACKNOWLEDGMENTS

This work was supported in part by Photonics Research, Ontario, the New Energy and Industrial Technology Development Organization (NEDO) of Japan, and the Natural Sciences and Engineering Research Council of Canada.

[1] A. Hasegawa and F. Tappert, Appl. Phys. Lett. **23**, 142 (1973).
[2] G. V. Agrawal, *Nonlinear Fiber Optics* (Academic Press, New York, 1995).
[3] H. G. Winful, J. H. Marburger, and E. Garmire, Appl. Phys. Lett. **35**, 379 (1979).
[4] W. Chen and D. L. Mills, Phys. Rev. Lett. **58**, 160 (1987).
[5] D. L. Mills and S. E. Trullinger, Phys. Rev. B **36**, 947 (1987).
[6] A. B. Aceves and S. Wabnitz, Phys. Lett. A **141**, 37 (1989).
[7] C. M. de Sterke and J. E. Sipe, in *Progress in Optics XXXIII*, edited by E. Wolf (Elsevier, Amsterdam, 1994), p. 203.
[8] S. John and N. Aközbek, Phys. Rev. Lett. **71**, 1168 (1993); N. Aközbek and S. John, Phys. Rev. E **57**, 2287 (1998).
[9] S. L. McCall and E. L. Hahn, Phys. Rev. Lett. **18**, 908 (1967); Phys. Rev. **183**, 457 (1969).
[10] G. L. Lamb, Jr., Rev. Mod. Phys. **43**, 99 (1971).
[11] R. E. Slusher, in *Progress in Optics XII*, edited by E. Wolf (Elsevier, Amsterdam, 1974).
[12] A. I. Maimistov, A. M. Basharov, S. O. Elyutin, and Yu. M. Sklyarov, Phys. Rep. **191**, 1 (1990).
[13] M. Nakazawa, Y. Kimura, K. Kurokawa, and K. Suzuki, Phys. Rev. A **45**, 23 (1992).
[14] M. Nakazawa, E. Yamada, and H. Kubota, Phys. Rev. Lett. **66**, 2625 (1991); Phys. Rev. A **44**, 5973 (1991).
[15] B. I. Mantsyzov and R. N. Kuzmin, Zh. Eksp. Teor. Fiz. **91**, 65 (1986) [Sov. Phys. JETP **64**, 37 (1986)]; B. I. Mantsyzov, Phys. Rev. A **51**, 4939 (1995).
[16] A. Kozhekin and G. Kurizki, Phys. Rev. Lett. **74**, 5020 (1995).
[17] L. Matulic and J. E. Eberly, Phys. Rev. A **6**, 822 (1972).
[18] S. John and V. I. Rupasov, Phys. Rev. Lett. **79**, 821 (1997).
[19] R. B. Boyd, *Nonlinear Optics*, 2nd ed. (Academic Press, San Diego, 1995).
[20] S. John and T. Quang, Phys. Rev. Lett. **76**, 2484 (1996); Phys. Rev. A **54**, 4479 (1996).
[21] M. A. Newbold and G. J. Salamo, Phys. Rev. Lett. **42**, 887 (1979).
[22] J. H. Eberly, Phys. Rev. Lett. **22**, 760 (1969).
[23] M. D. Crisp, Phys. Rev. Lett. **22**, 820 (1969).
[24] J. L. Shultz and G. J. Salamo, Phys. Rev. Lett. **78**, 855 (1997).

[25] P. F. Byrd and M. D. Friedman, *Handbook of Elliptic Integrals for Engineers and Scientists* (Springer, New York, 1971).
[26] C. De Angelis, IEEE J. Quantum Electron. **30**, 818 (1994).
[27] S. Cowan, R. H. Enns, S. S. Rangnekar, and S. S. Sanghera, Can. J. Phys. **64**, 311 (1986).
[28] L. Allen and J. H. Eberly, *Optical Resonance and Two-Level Atoms* (Dover, New York, 1987).
[29] C. M. Bowden, A. Postan, and R. Inguva, J. Opt. Soc. Am. B **8**, 1081 (1991).
[30] *Rare Earth Doped Fiber Lasers and Amplifiers*, edited by M. J. F. Digonnet (Dekker, New York, 1993).
[31] E. Desurvire, *Erbium-Doped Fiber Amplifiers* (Wiley, New York, 1994).